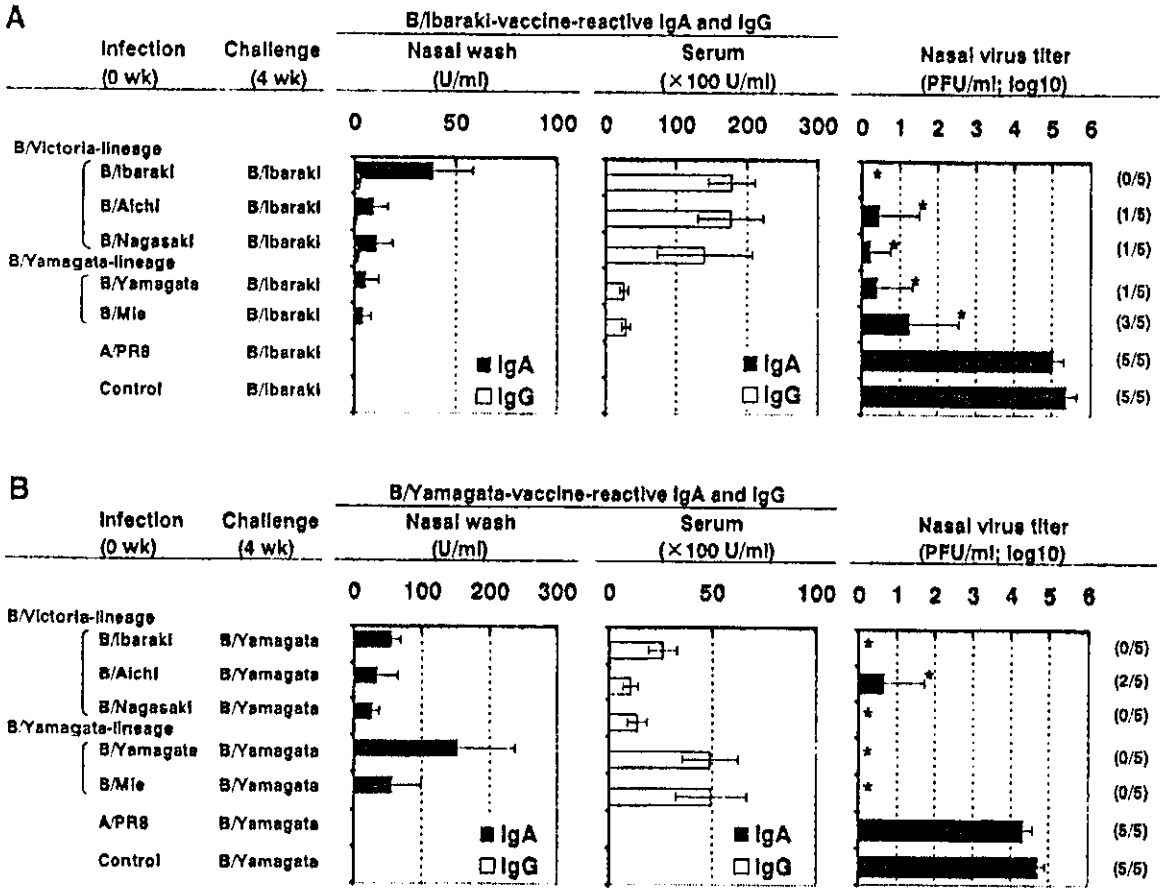

Fig. 1 B/Ibaraki or B/Yamagata vaccine-reactive antibody (Ab) responses and protection against (A) B/Ibaraki or (B) B/Yamagata virus infection in wild-type mice previously infected with different influenza B viruses, belonging to two antigenically distinct virus lineages; B/Victoria (B/Ibaraki, B/Aichi, and B/Nagasaki viruses) and B/Yamagata (B/Yamagata and B/Mie viruses), and challenged with B/Ibaraki or B/Yamagata viruses 4 weeks later. Three days after challenge, nasal wash and serum specimens from each group of five mice were obtained for B/Ibaraki or B/Yamagata vaccine-reactive IgA and IgG antibodies (Abs) titration and for B/Ibaraki or B/Yamagata virus titration as an index of protection. Each bar represents the mean B/Ibaraki or B/Yamagata vaccine-reactive IgA or IgG titer ± standard deviations (SD) in nasal wash or serum, or the mean virus titers (PFU/ml) ± SD in nasal wash. Mice with virus titers below the limit of detection (less than 5 PFU/ml) were considered to have cleared the infection, and a value of 0 was assigned for the purpose of statistical analysis. The specific protection afforded by the respective influenza B virus vaccines was compared with that due to A/PR8 vaccine. *Significantly different from the A/PR8 vaccine-immunized mice ($P < 0.05$). The values shown in parentheses are the numbers of mice that failed to clear nasal virus/total mice.

the efficacy of protection or cross-protection, mice were immunized i.n. with different CTB*-combined inactivated influenza B virus vaccines, prepared from B/Victoria-lineage viruses (B/Ibaraki, B/Aichi, and B/Nagasaki viruses) and B/Yamagata-lineage viruses (B/Yamagata and B/Mie viruses).

Four weeks after immunization, mice were challenged by upper respiratory tract infection with B/Ibaraki viruses. Three days after challenge, nasal wash and serum specimens were collected for virus and antibody titration. Immunization with B/Victoria-lineage virus vaccines conferred higher protection or cross-protection against the B/Ibaraki virus challenge than that with B/Yamagata-lineage virus vaccines (Fig. 2A). Each of these B virus vaccines gave significantly better protection or cross-protection against B/Ibaraki virus infection than A/PR8 vaccine or no immunization (Fig. 2A). This was consistent with the observation that immunization with B/Victoria-lineage virus vaccines induced higher B/Ibaraki vaccine-reactive IgA responses than immunization with B/Yamagata-lineage virus vaccines. Thus, the efficacy of protection or cross-protection correlated with the increase in nasal B/Ibaraki vaccine-reactive IgA titers, with a strong negative correlation between nasal virus shedding and nasal IgA titer ($r = -0.73$, $n = 35$). This result in mice previously immunized with different CTB*-combined inactivated B virus vaccines (Fig. 2A) is consistent with that in mice previously infected with various influenza B viruses (Fig. 1A).

To clarify the role of nasal IgA Abs in providing protection or cross-protection, B/Ibaraki vaccine-reactive IgA and IgG responses and protection against B/Ibaraki virus infection were examined in vaccinated pIgR-KO mice. Mice were immunized and challenged as described above. Immunization with B/Ibaraki, B/Aichi, B/Nagasaki, B/Yamagata, or B/Mie virus vaccines conferred low levels of protection or cross-protection against the challenge with B/Ibaraki virus (Fig. 2B). This low level of protection or cross-protection was accompanied by a reduction in the titer of nasal anti-B/Ibaraki

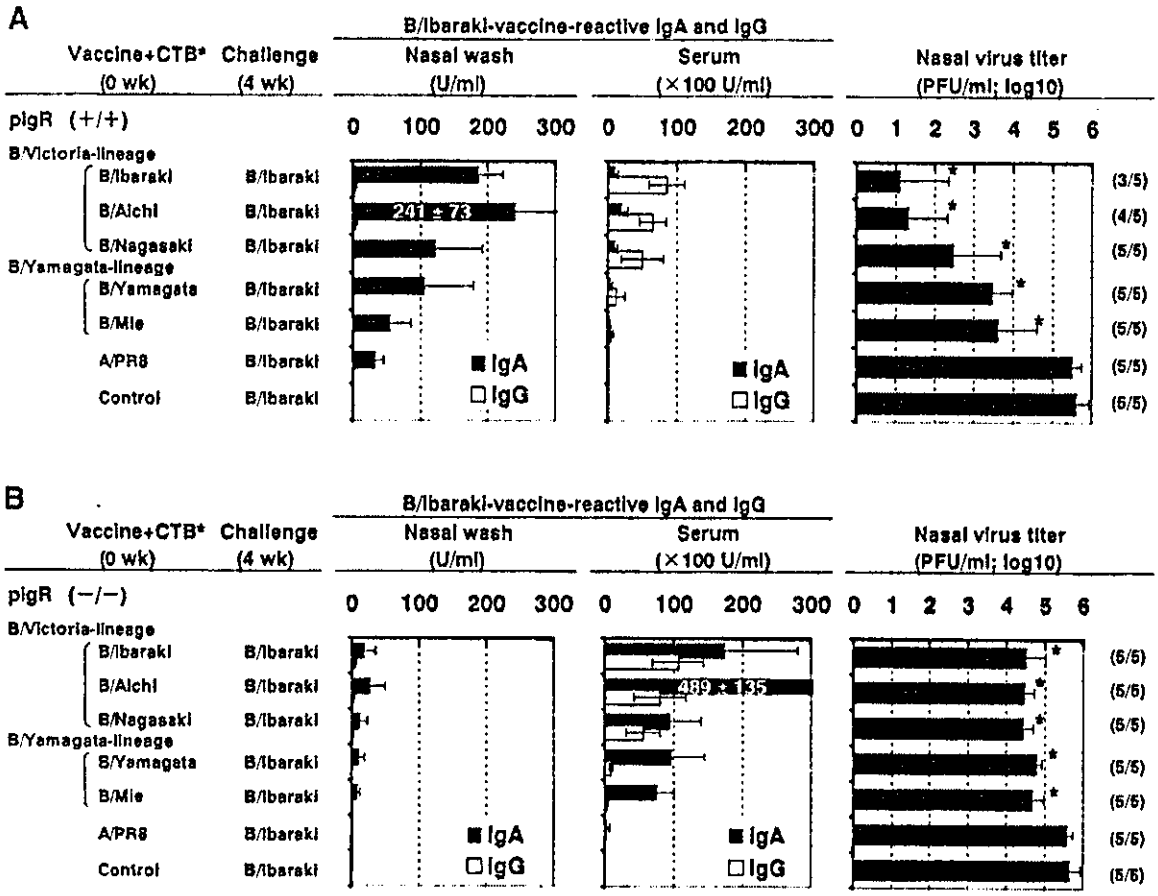

Fig. 2. B/Ibaraki vaccine-reactive Ab responses and protection against B/Ibaraki virus infection (A) in wild-type (polymeric Ig receptor (pIgR) +/+) and (B) in pIgR-knockout (KO) (pIgR −/−) mice immunized intranasal (i.n.) with CTB*-combined different inactivated influenza B virus vaccines, of antigenically distinct virus lineages, B/Victoria (B/Ibaraki, B/Aichi, and B/Nagasaki viruses) or B/Yamagata (B/Yamagata and B/Mie viruses), and challenged with the B/Ibaraki virus 4 weeks later. Three days after challenge, nasal wash and serum specimens from each group of five mice were obtained for B/Ibaraki vaccine-reactive IgA and IgG Abs titration and for B/Ibaraki virus titration as an index of protection. Each bar represents the mean B/Ibaraki vaccine-reactive IgA or IgG titer ± SD in nasal wash or serum, or the mean virus titers (PFU/ml) ± SD in nasal wash. For other details, see legend to Figure 1.

vaccine-reactive IgA Abs and by a marked increase the titer of serum anti-B/Ibaraki vaccine-reactive IgA Abs with no change in the serum IgG levels compared with wild-type mice (Fig. 2A). For the A/PR8 vaccine group, there was no non-specific influenza-type protection between the wild-type and pIgR-KO mice. These results clearly indicate that in pIgR-KO mice, the degree of protection or cross-protection provided by immunization with B/Ibaraki or other variant B virus vaccines was reduced in parallel with the reduction of nasal B/Ibaraki vaccine-reactive IgA Ab titers. There was a strong negative correlation between nasal virus shedding and nasal IgA titer (Fig. 2; $r = -0.80$, $n = 70$).

Ab Responses and Protection Against Upper Respiratory Tract Infection by B/Yamagata Viruses in Vaccinated Wild-Type and pIgR-KO Mice Immunized i.n. With Different Inactivated B Virus Vaccines

B/Yamagata vaccine-reactive IgA and IgG responses and protection against infection with B/Yamagata virus were examined in vaccinated wild-type and pIgR-KO mice. Mice were immunized with different CTB*-combined inactivated influenza B virus vaccines and challenged 4 weeks later with B/Yamagata viruses, as described above. Immunization with B/Victoria-lineage virus (B/Ibaraki, B/Aichi, and B/Nagasaki viruses) vaccines conferred a low level of cross-protection against challenge with B/Yamagata virus compared with complete protection or partial cross-protection conferred by immunization with B/Yamagata or B/Mie vaccines from B/Yamagata-lineage viruses. There was significantly better protection or cross-protection provided by each of these B virus vaccines compared with the A/PR8 vaccine and with non-immunized mice. The protective or cross-protective effect was associated with an enhanced nasal B/Yamagata vaccine-reactive IgA Ab response (Fig. 3A). This result in mice immunized with different CTB*-combined inactivated B virus vaccines (Fig. 3A) is roughly consistent with that in mice infected with various influenza B viruses (Fig. 1B).

Immunization with B/Ibaraki, B/Aichi, B/Nagasaki, B/Yamagata, or B/Mie vaccine in pIgR-KO mice (Fig. 3B)

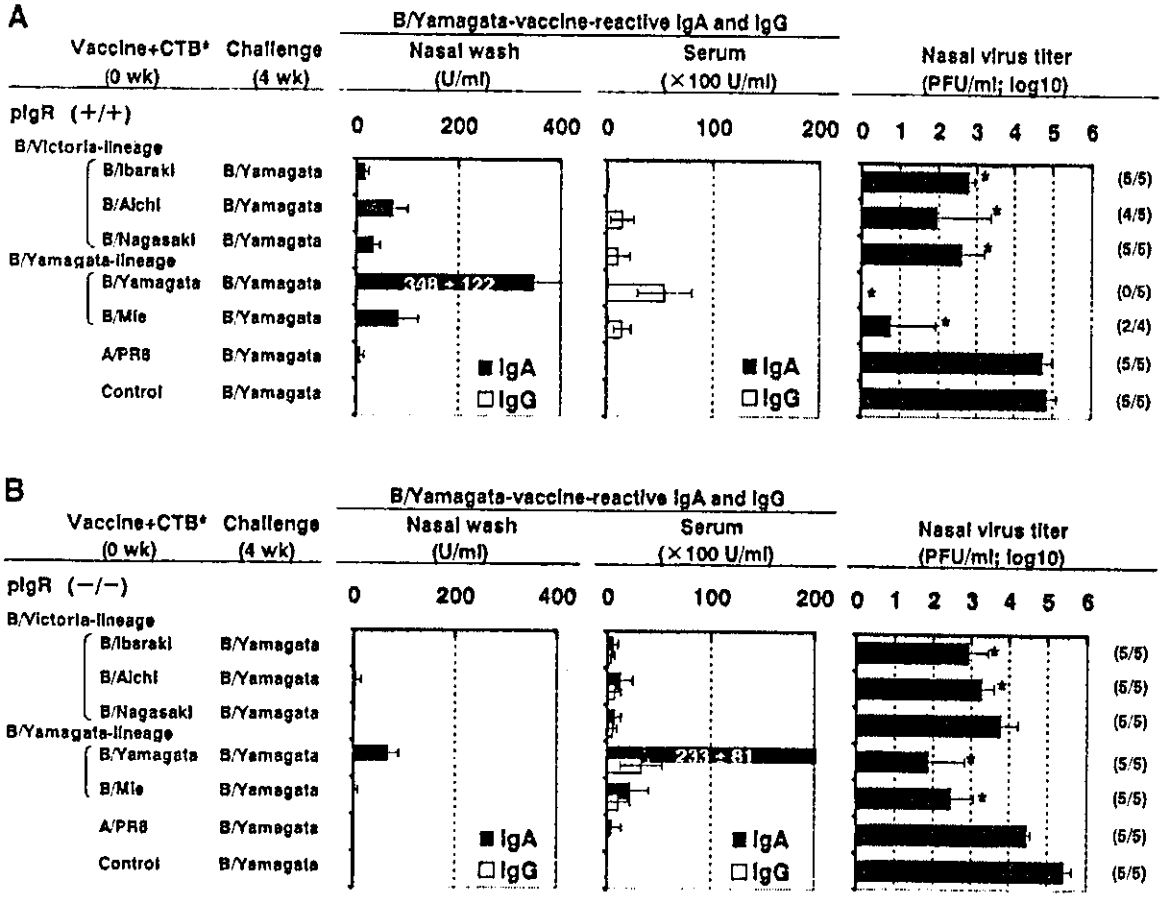

Fig. 3. B/Yamagata vaccine-reactive Ab responses and protection against B/Yamagata virus infection (A) in wild-type (pIgR +/+) and (B) in pIgR-KO (pIgR −/−) mice immunized with CTB*-combined different influenza B virus vaccines and challonged with the B/Yamagata virus 4 weeks later. Three days after the challenge, nasal wash and serum specimens were obtained for B/Yamagata vaccine-reactive IgA and IgG Abs titration and for B/Yamagata virus titration. For other details, see legend to Figure 1.

conferred partial protection or cross-protection against challenge with B/Yamagata virus, the efficacy of which was lower than in vaccinated wild-type mice (Fig. 3A). The lower level of protection or cross-protection in vaccinated pIgR-KO mice was contingent on a decrease in nasal anti-B/Yamagata vaccine-reactive IgA titer and on increases in serum IgA titer, (consistent with the results in Fig. 2A,B). Thus, the efficacy of protection or cross-protection against B/Ibaraki or B/Yamagata virus infection, provided by i.n. immunization with different B virus vaccines, was reduced in pIgR-KO mice compared with wild-type mice, and this reduction correlated with the reduction of nasal B/Ibaraki or B/Yamagata vaccine-reactive IgA titers. There was a strong negative correlation between nasal virus shedding and nasal B/Yamagata vaccine-reactive IgA titer (Fig. 3; $r = -0.68$, $n = 69$).

Taken together, these results suggest that S-IgA in the mucosal secretion of both B/Victoria- and B/Yamagata-lineage live virus or inactivated vaccine-immunized mice plays an essential role in providing cross-protection against challenge infection with either B/Victoria- or B/Yamagata-lineage virus.

DISCUSSION

This study examined the role of S-IgA antibodies in conferring cross-protective immunity against two antigenically distinct influenza B virus lineages, B/Victoria and B/Yamagata, in previously infected wild-type mice and previously vaccinated wild-type and pIgR-KO mice. Mice were challenged with either B/Ibaraki virus, of the B/Victoria-lineage, or B/Yamagata virus, of the B/Yamagata-lineage, 4 weeks post-immunization. The efficacy of protection or cross-protection correlated moderately or strongly with an increase in nasal B/Ibaraki (or B/Yamagata) vaccine-reactive IgA titers, in wild-type mice infected with various influenza B viruses (Fig. 1) or those immunized with different CTB*-combined inactivated B virus vaccines (Figs. 2A and 3A). In addition, in vaccinated pIgR-KO mice, there was no cross-protection against B/Ibaraki (or B/Yamagata) virus and there was a marked reduction of the nasal B/Ibaraki (or B/Yamagata) antigen cross-reactive IgA (Figs. 2B and 3B).

These results demonstrate that S-IgA reactive to the challenge virus induced by i.n. B virus infection or

vaccination, most strongly protects against upper respiratory tract infection with a homologous B virus, strongly protects against infection with drifted viruses within the homologous-lineage, and weakly protects against infection with heterologous-lineage viruses. These results are consistent with those previously described using a drifted virus within the H1N1 subtype of A virus [Asahi et al., 2002]. In contrast, Mbawuike et al. [1999] demonstrated that IgA is not required for protection against infection in IgA-KO mice immunized i.n. with a CTB*-combined A/PR8 vaccine and challenged with a lethal dose of A/PR8 virus. In their experiments, the role of IgA in cross-protection against heterologous virus infection in the upper respiratory tract, which is not due to serum IgG, remained to be determined. Our results suggest that there would be no cross-protection in IgA-KO mice against upper respiratory tract infection with variant influenza A or B viruses. We do not exclude the possibility that other protective mechanisms such as elevated IgM and IgG Ab titers, may be activated in IgA-KO mice.

In the current study, vaccine-reactive IgA and IgG Abs were assayed because they are essential components of protective immunity. Previously, it was reported that serum IgG and IgM levels were almost unaltered in both pIgR-KO and wild-type immunized mice, and that nasal IgM was a minor antibody [Asahi et al., 2002].

There was a lower degree of vaccine-reactive IgA Ab responses and a higher degree of protection or cross-protection in wild-type mice infected previously with different live viruses (Fig. 1A,B) compared with wild-type mice immunized previously with the different inactivated vaccines (Figs. 2A and 3A). These results could be explained by assuming that B virus-reactive antibodies, which are more effective in providing protection or cross-protection than inactivated B virus vaccine-reactive antibodies, could be involved in the protection or cross-protection in the previously infected mice. hus, the virus-reactive antibodies, induced by immunization with virus infection, contain more effective protective antibodies than the vaccine-reactive antibodies, which are induced by immunization with the ether and formalin-treated (split-product) vaccine. This notion seemed to be supported by the fact that the virus-reactive antibody titers were higher than the vaccine-reactive Ab titers in mice immunized with virus infection (data not shown).

Nasal immunization with B/Victoria- and the B/Yamagata-lineage virus vaccines conferred cross-protective immunity not only against homologous- but also heterologous-lineage virus infection in the upper respiratory tract of wild-type mice. The efficacy of cross-protection correlated with the degree of induction of S-IgA antibodies, which are cross-reactive to antigens of the challenge viruses. The degree of cross-reactive S-IgA induction seemed to depend on the antigenic similarity between vaccines and B/Ibaraki virus (Fig. 2A,B) or between vaccines and B/Yamagata virus (Fig. 3A,B), as reported previously [Kanegae et al., 1990; Kikuta et al., 1990; Rota et al., 1990]. These findings support the idea that mucosal administration of adjuvant-combined inactivated influenza vaccine, as well as live attenuated influenza vaccine, is important strategically [Tamura and Kurata, 1996]. The efficacy of the current parenteral vaccine would be improved by this approach, because mucosal vaccination induces cross-reactive S-IgA antibodies against drifted viruses within a subtype of A virus or within B virus, in addition to serum IgG antibodies which are induced by parenteral administration of inactivated vaccines.

REFERENCES

Asahi Y, Yoshikawa T, Watanabe I, Iwasaki T, Hasegawa H, Sato Y, Shimada S, Nanno M, Matsuoka Y, Ohwaki M, Iwakura Y, Suzuki Y, Aizawa C, Sata T, Kurata T, Tamura S. 2002. Protection against influenza virus infection in polymeric Ig receptor knockout mice immunized intranasally with adjuvant-combined vaccines. J Immunol 168:2930–2938.

Brandtzaeg P, Krajci P, Lamm ME, Kaetzel CS. 1994. Epithelial and hepatobiliary transport of polymeric immunoglobulins. In: Ogra PL, Mestecky J, Lamm ME, Strober W, McGhee JR, Bienenstock J, editors. Handbook of mucosal immunology. San Diego, CA: Academic Press. pp 113–126.

Clements ML, O'Donnell S, Levine MM, Chanock RM, Murphy BR. 1983. Dose response of A/Alaska/6/77 (H3N2) cold-adapted reassortant vaccine virus in adult volunteers: Role of local antibody in resistance to infection with vaccine virus. Infect Immun 40:1044–1051.

Couch RB, Kasel JA. 1983. Immunity to influenza in man. Annu Rev Microbiol 37:529–549.

Davenport FM, Hennessy AV, Brandon FM, Webster RG, Barrett CD, Jr., Lease GO. 1964. Comparison of serologic and febrile responses in humans to vaccination with influenza A viruses or their hemagglutinin. J Lab Clin Med 63:5–13.

Hall CE, Cooney MK, Fox JP. 1973. The Seattle virus watch. IV. Comparative epidemiologic observations of infections with influenza A and B viruses, 1965–1969, in families with young children. Am J Epidemiol 98:365–380.

Housworth J, Langmuir AD. 1974. Excess mortality from epidemic influenza, 1957–1966. Am J Epidemiol 100:40–48.

Johnson PR, Feldman S, Thompson JM, Mahoney JD, Wright PF. 1986. Immunity to influenza A virus infection in young children: A comparison of natural infection, live cold-adapted vaccine, and inactivated vaccine. J Infect Dis 154:121–127.

Kanegae Y, Sugita S, Endo A, Ishida M, Senya S, Osako K, Nerome K, Oya A. 1990. Evolutionary pattern of the hemagglutinin gene of influenza B viruses isolated in Japan: Cocirculating lineages in the same epidemic season. J Virol 64:2860–2865.

Kikuta K, Hirabayashi Y, Nagamine T, Aizawa C, Ueno Y, Oya A, Kurata T, Tamura S. 1990. Cross-protection against influenza B type virus infection by intranasal inoculation of the HA vaccines combined with cholera toxin B subunit. Vaccine 8:595–599.

Kris RM, Asofsky R, Evans CB, Small PAJ. 1985. Protection and recovery in influenza virus-infected mice immunosuppressed with anti-IgM. J Immunol 134:1230–1235.

Liew FY, Russell SM, Appleyard G, Brand CM, Beale J. 1984. Cross-protection in mice infected with influenza A virus by the respiratory route is correlated with local IgA antibody rather than serum antibody or cytotoxic T cell reactivity. Eur J Immunol 14:350–356.

Mbawuike IN, Pacheco S, Acuna CL, Switzer KC, Zhang Y, Harriman GR. 1999. Mucosal immunity to influenza without IgA: An IgA knockout mouse model. J Immunol 162:2530–2537.

Mostov KE, Deitcher DL. 1986. Polymeric immunoglobulin receptor expressed in MDCK cells transcytoses IgA. Cell 46:613–621.

Murphy BR. 1994. Mucosal immunity to viruses. In: Ogra PL, Mestecky J, Lamm ME, Strober W, McGhee JR, Bienenstock J, editors. Handbook of mucosal immunology. San Diego, CA: Academic Press. pp 333–343.

Murphy BR, Clements ML. 1989. The systemic and mucosal immune response of humans to influenza A virus. Curr Top Microbiol Immunol 146:107–116.

Murphy BR, Webster RG. 1996. Fields virology. In: Fields BN, Knipe DN, Howley PM, editors Philadelphia: Lippincott Raven Publishers. pp 1397–1445.

Ramphal R, Cogliano RC, Shands JWJ, Small PAJ. 1979. Serum antibody prevents lethal murine influenza pneumonitis but not tracheitis. Infect Immun 25:992–997.

Renegar KB, Small PAJ. 1994. Passive immunization: Systemic and mucosal. In: Ogra PL, Mestecky J, Lamm ME, Strober W, McGhee JR, Bienenstock J, editors. Handbook of mucosal immunology San Diego, CA: Academic Press. pp 347–356.

Rota PA, Wallis TR, Harmon MW, Rota JS, Kendal AP, Nerome K. 1990. Cocirculation of two distinct evolutionary lineages of influenza type B virus since 1983. Virology 175:59–68.

Shimada S, Kawaguchi-Miyashita M, Kushiro A, Sato T, Nanno M, Sako T, Matsuoka Y, Sudo K, Tagawa Y, Iwakura Y, Ohwaki M. 1999. Generation of polymeric immunoglobulin receptor-deficient mouse with marked reduction of secretory IgA. J Immunol 163: 5367–5373.

Song W, Bomsel M, Casanova J, Vaerman JP, Mostov K. 1994. Stimulation of transcytosis of the polymeric immunoglobulin receptor by dimeric IgA. Proc Natl Acad Sci USA 91:163–166.

Tamer CM, Lamm ME, Robinson JK, Piskurich JF, Kaetzel CS. 1995. Comparative studies of transcytosis and assembly of secretory IgA in Madin–Darby canine kidney cells expressing human polymeric Ig receptor. J Immunol 155:707–714.

Tamura SI, Kurata T. 1996. Intranasal immunization with influenza vaccine. In: Kiyono H, Ogra PL, McGhee JR, editors. Mucosal vaccines. San Diego, CA: Academic Press. pp 425–436.

Tamura S, Samegai Y, Kurata H, Nagamine T, Aizawa C, Kurata T. 1988 Protection against influenza virus infection by vaccine inoculated intranasally with cholera toxin B subunit. Vaccine 6: 409–413.

Tamura S, Asanuma H, Ito Y, Hirabayashi Y, Suzuki Y, Nagamine T, Aizawa C, Kurata T, Oya A. 1992a. Superior cross-protective effect of nasal vaccination to subcutaneous inoculation with influenza hemagglutinin vaccine. Eur J Immunol 22:477–481.

Tamura S, Ito Y, Asanuma H, Hirabayashi Y, Suzuki Y, Nagamine T, Aizawa C, Kurata T. 1992b. Cross-protection against influenza virus infection afforded by trivalent inactivated vaccines inoculated i.n. with cholera toxin B subunit. J Immunol 149:981–988.

Tamura S, Yamanaka A, Shimohara M, Tomita T, Komase K, Tsuda Y, Suzuki Y, Nagamine T, Kawahara K, Danbara H. 1994. Synergistic action of cholera toxin B subunit (and *Escherichia coli* heat-labile toxin B subunit) and a trace amount of cholera whole toxin as an adjuvant for nasal influenza vaccine. Vaccine 12:419–426.

Tamura S, Miyata K, Matsuo K, Asanuma H, Takahashi H, Nakajima K, Suzuki Y, Aizawa C, Kurata T. 1996. Acceleration of influenza virus clearance by Th1 cells in the nasal site of mice immunized intranasally with adjuvant-combined recombinant nucleoprotein. J Immunol 156:3892–3900.

Tobita K. 1975. Permanent canine kidney (MDCK) cells for isolation and plaque assay of influenza B viruses. Med Microbiol Immunol (Berl) 162:23–27.

Tobita K, Sugiura A, Enomote C, Furuyama M. 1975. Plaque assay and primary isolation of influenza A viruses in an established line of canine kidney cells (MDCK) in the presence of trypsin. Med Microbiol Immunol (Berl) 162:9–14.

Yetter RA, Lehrer S, Ramphal R, Small PAJ. 1980. Outcome of influenza infection: Effect of site of initial infection and heterotypic immunity. Infect Immun 29:654–662.

TNF-α is crucial for the development of autoimmune arthritis in IL-1 receptor antagonist–deficient mice

Reiko Horai,[1,2] Akiko Nakajima,[1] Katsuyoshi Habiro,[3] Motoko Kotani,[3] Susumu Nakae,[1] Taizo Matsuki,[1] Aya Nambu,[1] Shinobu Saijo,[1] Hayato Kotaki,[1] Katsuko Sudo,[1] Akihiko Okahara,[4] Hidetoshi Tanioka,[4] Toshimi Ikuse,[4] Naoto Ishii,[5] Pamela L. Schwartzberg,[2] Ryo Abe,[3] and Yoichiro Iwakura[1]

[1]Center for Experimental Medicine, Institute of Medical Science, University of Tokyo, Tokyo, Japan. [2]National Human Genome Research Institute, NIH, Bethesda, Maryland, USA. [3]Research Institute for Biological Sciences, Tokyo University of Science, Chiba, Japan. [4]Santen Pharmaceutical Co., Osaka, Japan. [5]Department of Microbiology and Immunology, Tohoku University Graduate School of Medicine, Sendai, Japan.

IL-1 receptor antagonist–deficient (IL-1Ra$^{-/-}$) mice spontaneously develop autoimmune arthritis. We demonstrate here that T cells are required for the induction of arthritis; T cell–deficient IL-1Ra$^{-/-}$ mice did not develop arthritis, and transfer of IL-1Ra$^{-/-}$ T cells induced arthritis in *nu/nu* mice. Development of arthritis was also markedly suppressed by TNF-α deficiency. We found that TNF-α induced OX40 expression on T cells and blocking the interaction between either CD40 and its ligand or OX40 and its ligand suppressed development of arthritis. These findings suggest that IL-1 receptor antagonist deficiency in T cells disrupts homeostasis of the immune system and that TNF-α plays an important role in activating T cells through induction of OX40.

Introduction

RA is a systemic, chronic, inflammatory disorder exhibited most commonly in the joints. Although various factors including genetic factors, environmental factors, and infectious agents have been suggested as causes of the disease (1), so far the etiology and pathogenesis have not been completely elucidated. Patients often produce autoantibodies against various self components such as IgGs, type II collagen, and nuclear antigens, suggesting an autoimmune nature of the disease (2). Many proinflammatory cytokines, including IL-1 and TNF-α, chemokines, and growth factors, are expressed in diseased joints, forming a complex cytokine network. It is widely believed that dysregulation of the cytokine network contributes to the pathogenesis of RA (3).

IL-1 is a prototype proinflammatory cytokine and is produced by various types of cells, including monocytes/macrophages, lymphocytes, and synovial lining cells (4). Since IL-1 induces inflammation, promotes synovial cell growth, and promotes differentiation of osteoclasts, an important role for this cytokine in the development of RA has been suggested (1, 5). IL-1 receptor antagonist (IL-1Ra) is an endogenous inhibitor of IL-1. IL-1Ra production is induced by a number of other cytokines, viral products, and acute-phase proteins and is augmented in patients with autoimmune and inflammatory diseases, suggesting that IL-1Ra may play regulatory roles in these diseases (6). TNF-α is also thought to be importantly involved in the inflammation and bone destruction in RA. TNF-α is produced mainly by monocytes/macrophages, which are activated by soluble components of bacteria and by direct contact with activated T cells at inflammatory sites. The production of IL-1 is coordinated with that of TNF-α, and they mutually stimulate each other's production. Overproduction of these cytokines by gene manipulation has been found to predispose the organism to inflammatory arthritis (7–10).

Cumulative evidence suggests that T cell–mediated autoimmune responses play a crucial role in the pathogenesis of RA. In fact, it has been demonstrated that T cells from RA patients can cause inflammatory arthritis in SCID mice (11). T cells that invade tissues and cause autoimmune destruction express activation antigens that are not expressed on normal resting T cells. These activation antigens include the IL-2 receptor α (CD25), CD69, CD44, CD40 ligand (CD40L; also known as CD154), and OX40 (also known as CD134) (12) CD40L on T cells and its receptor on APCs, as well as OX40 on T cells and its ligand (OX40L) on APCs, generate costimulatory signals that enhance T cell proliferation and cytokine production. Indeed, the expression of OX40 on T cells in rheumatoid synovial tissues is quite pronounced in some patients (12), and blocking either CD40L or OX40L in vivo reduces the severity of collagen-induced arthritis (CIA), experimental allergic encephalomyelitis, and inflammatory bowel disease in animal models of these diseases (13, 14). However, the molecular mechanisms for the induction of these costimulatory molecules in RA are not fully understood. We previously reported that IL-1 plays an important role in enhancing T cell–APC interactions through induction of CD40L and OX40 on T cells (15). Thus, excess IL-1 signaling may activate these pathways, leading to the development of T cell–mediated autoimmune diseases.

We previously reported that IL-1Ra$^{-/-}$ mice on the BALB/c background spontaneously develop chronic inflammatory arthropathy (9). Histopathology showed marked synovial and periarticular inflammation, with articular erosion caused by invasion of granulation tissues closely resembling that of RA in humans. Moreover, elevated levels of antibodies against immunoglobulins (rheumatoid factor [RF]), type II collagen, and double-stranded DNA were detected in sera of these mice, consistent with the development

Nonstandard abbreviations used: CD40L, CD40 ligand; CIA, collagen-induced arthritis; IL-1Ra, IL-1 receptor antagonist; PEC, peritoneal exudate cells; RF, rheumatoid factor.

Conflict of interest: The authors have declared that no conflict of interest exists.

Citation for this article: *J. Clin. Invest.* 114:1603–1611 (2004). doi:10.1172/JCI200420742.

Table 1
Incidence of arthritis in IL-1Ra$^{-/-}$ *scid/scid* mice

Genotype of *scid* loci	Incidence (%)
scid/scid	0/6 (0%)[A]
scid/+	9/11 (82%)
+/+	7/8 (88%)

Incidence of arthritis was judged at 20 weeks of age. Development of arthritis was completely suppressed in T cell–deficient IL-1Ra$^{-/-}$ *scid/scid* mice. [A]$P < 0.01$ by chi-square for independence test.

of autoimmunity. Proinflammatory cytokines such as IL-1β, IL-6, and TNF-α were overexpressed in the joints, indicating regulatory roles of IL-1Ra in the cytokine network. These data therefore suggested that IL-1Ra is crucial for the homeostasis of the immune system. It is not known, however, which cells in the immune system are crucial for the regulation of IL-1 and its actions, or furthermore, which cytokines are involved in the pathogenesis of arthritis in this model.

In this study, to elucidate the pathogenesis of the autoimmune arthritis in IL-1Ra$^{-/-}$ mice, we assessed the role of T cells in the development of arthritis by transferring T cells from IL-1Ra$^{-/-}$ mice to *nu/nu* mice and by intercrossing IL-1Ra$^{-/-}$ mice with T cell–deficient mice. We show that IL-1Ra$^{-/-}$ deficiency in T cells is enough for the development of arthritis. Furthermore, we analyzed the role of TNF-α in this model by producing TNF-α$^{-/-}$ IL-1Ra$^{-/-}$ mice, and we were able to demonstrate that TNF-α is crucial for the development of arthritis, as it induces OX40 on T cells. Treatment with anti-CD40L or anti-OX40L Ab suppressed disease, demonstrating the importance of CD40-CD40L and OX40-OX40L interactions for the development of autoimmune arthritis.

Results

Development of arthritis is suppressed in T cell– and B cell–deficient IL-1Ra$^{-/-}$ mice. IL-1Ra$^{-/-}$ mice on the BALB/c background spontaneously developed chronic inflammatory arthritis. Since high levels of RF, antibody to type II collagen, and antibody to double-stranded DNA are observed in IL-1Ra$^{-/-}$ mice, we hypothesized that there could be an autoimmune mechanism for the pathogenesis. To address this question, we evaluated the contribution of T cells and/or B cells to the development of arthritis in IL-1Ra$^{-/-}$ mice by intercrossing them with *scid/scid* mice on the BALB/c background. While IL-1Ra$^{-/-}$ *scid/+* or IL-1Ra$^{-/-}$ *+/+* mice showed a high incidence of arthritis, IL-1Ra$^{-/-}$ *scid/scid* mice failed to develop arthritis by 20 weeks of age (Table 1). These results suggest that combined deficiency of T and B cells completely suppresses the development of arthritis in IL-1Ra$^{-/-}$ mice.

Peripheral T cells from IL-1Ra$^{-/-}$ mice induced arthritis. We next examined the contribution of the specific cell types of the immune system to the development of arthritis by cell transfer experiments. When total splenocytes from IL-1Ra$^{-/-}$ mice were transferred into *nu/nu* mice on the BALB/c background, these mice developed severe arthritis as early as 3 weeks after the cell transfer (Figure 1, A and B). On the other hand, when T cell–depleted splenocytes were transferred into *nu/nu* mice, these mice did not develop arthritis at all. These results strongly suggest that T cells are involved in the development of arthritis. We further examined the effects of transplantation of purified T cells in the periphery. When T cells from spleens and LNs were transferred into *nu/nu* mice, they developed severe arthritis as early as 2 weeks after transfer (Figure 1, C and D). The disease status of the donor mice influenced these results; T cells from arthritic mice were more efficient than those

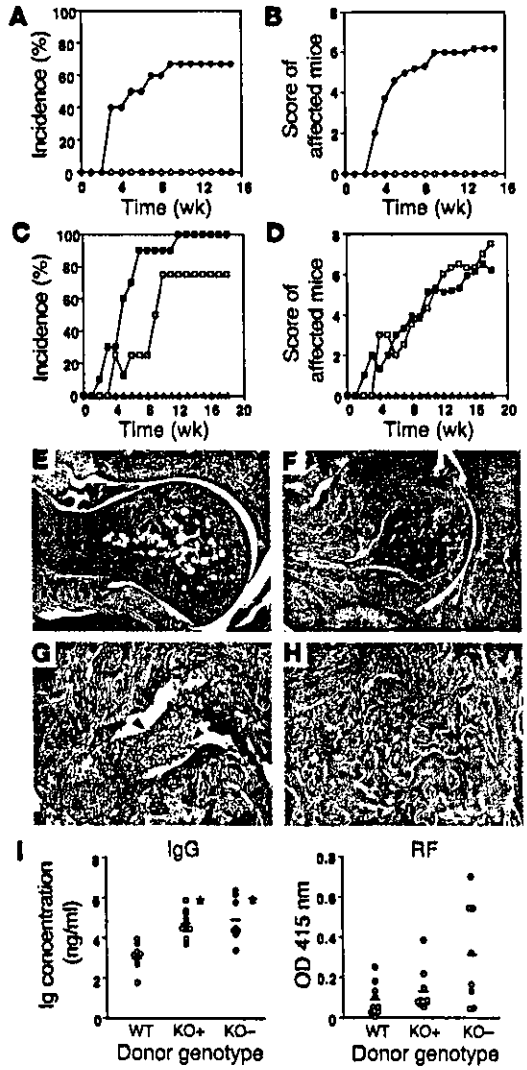

Figure 1
Splenocyte and T cell transfer into *nu/nu* mice. (**A**) Total splenocytes from IL-1Ra$^{-/-}$ mice (filled circles, $n = 10$) induced arthritis, while T cell–depleted splenocytes (open circles, $n = 7$) did not induce arthritis in *nu/nu* mice. (**B**) Arthritic severity score of splenocyte-transferred mice. (**C**) Purified T cells from spleen and LNs of either arthritic (filled squares, $n = 10$) or nonarthritic (open squares, $n = 8$) IL-1Ra$^{-/-}$ mice induced arthritis in *nu/nu* mice, while T cells from WT mice (triangles, $n = 11$) did not. (**D**) Arthritic severity score of T cell–transferred mice. (**E–H**) Histology of the ankle joints of WT (**E**) or IL-1Ra$^{-/-}$ (**F–H**) T cell–transferred *nu/nu* mice. (**G**) Infiltration of inflammatory cells (indicated by arrowheads). (**H**) Erosive bone destruction by replacement of bone matrix with fibroblastic cells (indicated by arrowheads). Magnification, ×40 (**E** and **F**); ×100 (**G** and **H**). (**I**) Serum IgG (left) and RF (right) levels in WT T cell– or IL-1Ra$^{-/-}$ T cell–transferred *nu/nu* mice. The average in each group is shown as a horizontal bar. WT, WT donors ($n = 10$); KO+, arthritic-IL-1Ra$^{-/-}$ donors ($n = 10$); KO–, nonarthritic IL-1Ra$^{-/-}$ donors ($n = 8$). $^*P < 0.05$.

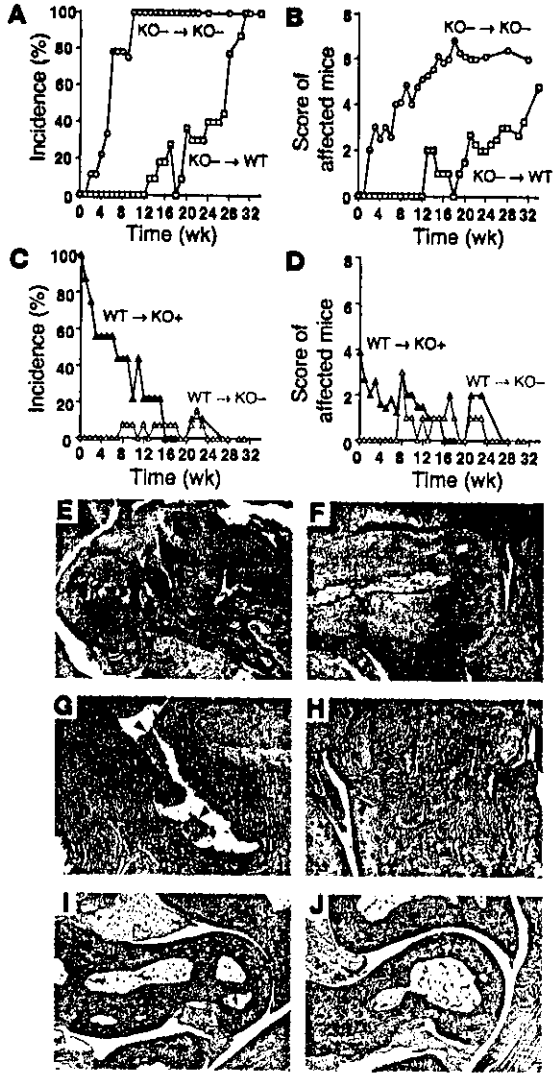

Figure 2
BM cell replacement between WT and IL-1Ra$^{-/-}$ mice. BM cells from IL-1Ra$^{-/-}$ mice induced arthritis in WT mice, while those from WT mice suppressed arthritis in IL-1Ra$^{-/-}$ mice. (**A**) Incidence of arthritis in IL-1Ra$^{-/-}$ BM cell–transferred WT (squares, $n = 11$) or IL-1Ra$^{-/-}$ mice (circles, $n = 9$). (**B**) Arthritic severity score of IL-1Ra$^{-/-}$ BM cell–transferred mice. (**C**) Incidence of arthritis in WT BM cell–transferred IL-1Ra$^{-/-}$ mice with (closed triangle, $n = 9$) or without (open triangle, $n = 13$) arthritis. (**D**) Arthritic severity score of WT BM–transferred IL-1Ra$^{-/-}$ mice. (**E–H**) Histopathology of the ankle joints of IL-1Ra$^{-/-}$ BM cell–transferred IL-1Ra$^{-/-}$ mice (**E**) and IL-1Ra$^{-/-}$ BM cell–transferred WT mice (**F–H**) at the end of the experiments (32 weeks and 34 weeks after the cell transfer, respectively). (**G**) Infiltration of inflammatory cells (indicated by arrowheads) into articular space and proliferation of the lining cells of the synovial membrane. (**H**) Pannus formation and erosive destruction of the bone (indicated by arrowheads). (**I** and **J**) Histology of the normal ankle joints of WT BM cell–transferred nonarthritic IL-1Ra$^{-/-}$ mice (**I**) and arthritic IL-1Ra$^{-/-}$ mice (**J**) at 31 weeks after the cell transfer. Magnification, ×40 (**E**, **F**, **I**, and **J**); ×100 (**G** and **H**).

from nonarthritic mice in inducing arthritis in recipient mice (Figure 1C). However, cells from both arthritic and nonarthritic mice could induce the disease. Histological analyses revealed that arthritis was observed in both ankle and knee joints of IL-1Ra$^{-/-}$ T cell–transferred *nu/nu* mice (Figure 1, F–H and data not shown). Proliferation of synovial cells, infiltration of neutrophils and lymphocytes, and bone destruction were remarkable in both ankle and knee joints (Figure 1, E–H and data not shown). Serum IgG levels and RF levels were enhanced in IL-1Ra$^{-/-}$ T cell–transferred *nu/nu* mice compared with WT T cell–transferred mice, although the difference in RF levels was not statistically significant (Figure 1I). We also performed thymocyte transfer experiments to examine whether or not activation of IL-1Ra$^{-/-}$ T cells before transplantation is necessary, and we found that thymocytes from IL-1Ra$^{-/-}$ mice induced arthritis in *nu/nu* mice, but with lower frequency than that seen in mice transferred with splenocytes or purified T cells (IL-1Ra$^{-/-}$ thymocyte–transferred mice, 46%; WT thymocyte–transferred mice, 0% at 15 weeks). These results clearly indicate that T cells are required for the development of arthritis in IL-1Ra$^{-/-}$ mice, and suggest that IL-1Ra$^{-/-}$ T cells can enhance immune responses against self components.

BM-derived cells from IL-1Ra$^{-/-}$ mice induced arthritis in normal mice and those from normal mice suppressed the development of arthritis in IL-1Ra$^{-/-}$ mice. To examine whether abnormal T cell education or a stem cell disorder is responsible for the T cell abnormality seen in IL-1Ra$^{-/-}$ mice, we next reconstituted the immune system by BM cell transfers. BM cells were prepared from IL-1Ra$^{-/-}$ mice by treating these cells with anti-Thy-1.2 Ab to deplete T cells, and then they were transferred into the recipient mice that were lethally irradiated. Mice that received BM cells did not die, whereas those that did not receive BM cells died within 2 weeks. We observed the development of arthritis as early as 2 weeks after the transfer of 4-week-old IL-1Ra$^{-/-}$ BM cells to nonarthritic IL-1Ra$^{-/-}$ mice, which would normally develop arthritis at 5–8 weeks of age (Figure 2A). Arthritis was also observed in WT mice receiving IL-1Ra$^{-/-}$ BM cells. These mice developed arthritis, however, more than 3 months after the transfer, indicating that the genotype of recipient mice (WT or IL-1Ra–deficient) affects the incidence and severity of arthritis (Figure 2, A and B). Replacement of the recipient BM cells by the donor cells was confirmed by Southern blot analyses at the end of the experiments. Cells from lymphoid tissues such as the spleen and LNs consisted mainly of the donor cells, while those from joints showed both donor and recipient genotypes (data not shown), suggesting that only BM-derived cells were replaced in the joints (16). Histological analysis of the ankle joints showed synovial and periarticular inflammation with articular erosion in both WT and IL-1Ra$^{-/-}$ mice that received IL-1Ra$^{-/-}$ BM cells (Figure 2, E and F). We observed proliferation of synovial lining cells and invasion of inflammatory cells, includ-

Table 2
Increased cytokine secretion by CD4$^+$ T cells from IL-1Ra$^{-/-}$ mice

Cytokine	Detection limit	WT	IL-1Ra$^{-/-}$
IFN-γ (U/ml)	20 U/ml	59.7 ± 13.0	153.8 ± 19.1^A
IL-4 (pg/ml)	10 pg/ml	42.0 ± 5.0	161.9 ± 3.2^A
TNF-α (pg/ml)	12.5 pg/ml	52.0 ± 7.8	95.3 ± 3.7^A

Purified CD4$^+$ T cells were stimulated with 1 μg/ml (IFN-γ and IL-4) or 10 μg/ml (TNF-α) of plate-coated anti-CD3 mAb for 48 hours. Data are expressed as mean ± SEM ($n = 4$). $^AP < 0.01$ by Student's t test. Similar results were obtained from 2 independent experiments.

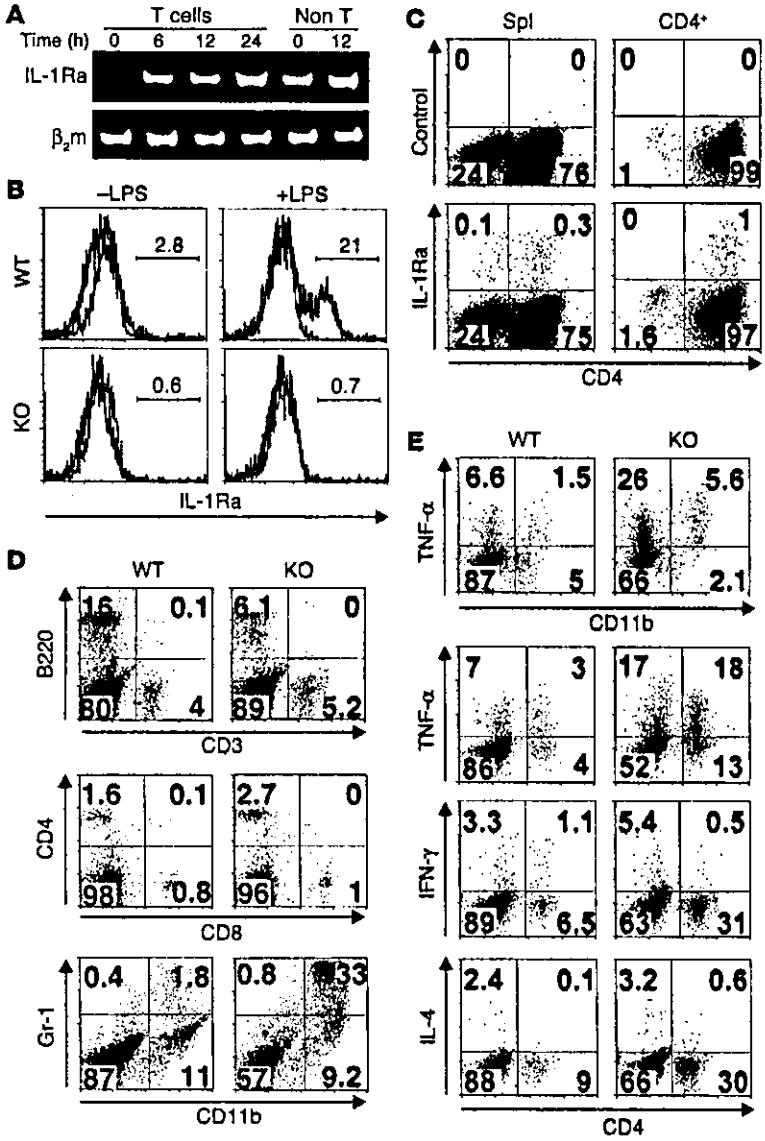

Figure 3
IL-1Ra and cytokine production. (**A**) *IL-1Ra* mRNA expression in WT T cells. Purified T cells from WT mice were stimulated with 10 μg/ml of plate-coated anti-CD3 mAb for 0, 6, 12, or 24 hours, and *IL-1Ra* mRNA levels were determined by RT-PCR. T cell–depleted splenocytes (Non T) were stimulated with 5 μg/ml LPS for 0 and 12 hours as controls. β_2m is used as an internal control. (**B**) Intracellular staining for IL-1Ra in PECs. PECs from WT and IL-1Ra$^{-/-}$ mice were stimulated with LPS, and IL-1Ra$^+$ cells in the CD11b$^+$ population are shown as histograms. Black-lined histograms: staining with IL-1Ra Ab. Gray-lined histograms: staining with isotype control Ig. Percentages of IL-1Ra$^+$ cells are indicated. (**C**) Intracellular staining for IL-1Ra in splenocytes (Spl) and CD4$^+$ T cells from WT mice after stimulation with anti-CD3 mAb. Upper panels show staining with isotype control Ig and lower panels show staining with anti–IL-1Ra Ab. (**D**) Expression of cell lineage–specific surface molecules on cells from ankle joints of WT and IL-1Ra$^{-/-}$ (KO) mice. B220, Gr-1, and CD11b are markers for B cells, granulocytes (including neutrophils), and macrophages, respectively. (**E**) Intracellular staining for cytokines in cells from the ankle joints of WT and IL-1Ra$^{-/-}$ mice. Joint-derived cells were stimulated with 10 ng/ml PMA and 400 ng/ml ionomycin for 6 hours with 2 μM monensin. Similar results were obtained in 3 independent experiments.

ing lymphocytes and neutrophils (Figure 2, E–G). Bone erosion and pannus formation were also remarkable (Figure 2H).

To examine whether normal stem cells can suppress the development of arthritis in IL-1Ra$^{-/-}$ mice, we prepared BM cells from WT mice and transferred them into irradiated nonarthritic or arthritic IL-1Ra$^{-/-}$ mice. Development of arthritis was suppressed in nonarthritic IL-1Ra$^{-/-}$ mice that received normal BM cells (Figure 2, C and D). Arthritis was also ameliorated in arthritic IL-1Ra$^{-/-}$ mice that received normal BM cells (Figure 2, C and D). At 31 weeks after transfer of BM cells, joint pathology was examined histologically. Nonarthritic IL-1Ra$^{-/-}$ mice that received normal BM cells showed no sign of arthritis (Figure 2I). Moreover, arthritic IL-1Ra$^{-/-}$ mice that received normal BM cells showed complete recovery from arthritis (Figure 2J). Thus, replacement of the BM-derived cells in IL-1Ra$^{-/-}$ mice with those of normal mice can suppress and actually reverse the development of arthritis in IL-1Ra$^{-/-}$ mice. These results indicate that BM-derived cells themselves are abnormal in IL-1Ra$^{-/-}$ mice.

Enhanced cytokine production from activated T cells in IL-1Ra$^{-/-}$ mice. Since our results suggested abnormal T cell function in IL-1Ra$^{-/-}$ mice, we next analyzed T cell proliferation and cytokine production upon TCR stimulation. Proliferative responses of T cells from IL-1Ra$^{-/-}$ mice stimulated with anti-CD3 mAb were normal (data not shown). However, these T cells produced much higher levels of IFN-γ, IL-4, and TNF-α in the culture supernatant than did those from WT mice (Table 2). These results suggest that IL-1Ra$^{-/-}$ T cells produce higher levels of cytokines upon TCR stimulation.

We also examined IL-1Ra expression in normal WT T cells by RT-PCR, ELISA, and intracellular staining. Unstimulated T cells expressed low levels of *IL-1Ra* mRNA, but upon stimulation through TCR, *IL-1Ra* mRNA expression was upregulated (Figure 3A). We also observed secretion of the IL-1Ra protein in the culture supernatant of WT purified CD4$^+$ T cells (>99% purity) after anti-CD3 mAb stimulation (20–40 pg/ml at 72–96 hours), indicating that T cells can produce and secrete the IL-1Ra protein. To confirm the IL-1Ra protein production from T cells directly, we stained stimulated CD4$^+$ T cells intracellularly with anti-IL-1Ra Ab. As a control experiment for the staining, we first stained peritoneal exudate cells (PECs) from WT or IL-1Ra$^{-/-}$ mice stimulated with or without LPS, and showed that the staining specifically detected IL-1Ra after the stimulation (Figure 3B). Then, purified CD4$^+$ T cells from BALB/c WT mice were stimulated with plate-coated anti-CD3 mAb and stained for the intracellular IL-1Ra protein. As shown in Figure 3C, CD4$^+$ T cells can produce IL-1Ra protein after TCR stimulation. These IL-1Ra–producing cells were different from those which produce IFN-γ, IL-4, or IL-10 under these conditions (data not shown). These results indicate that IL-1Ra is produced by T cells and may regulate T cell activation by IL-1.

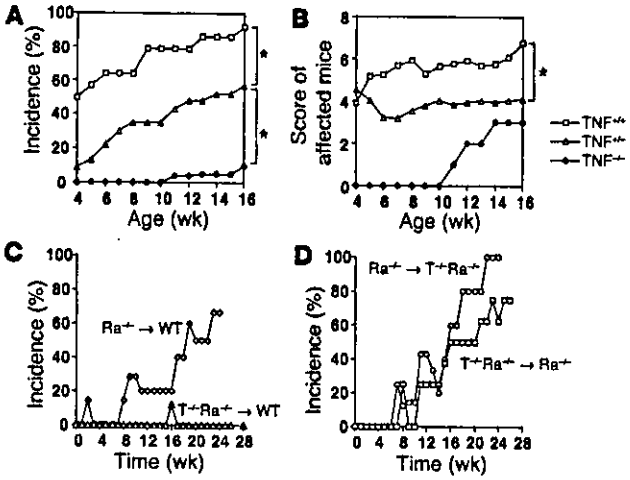

Figure 4

Incidence of arthritis in TNF-α–deficient IL-1Ra$^{-/-}$ mice. Incidence (**A**) and severity score (**B**) of arthritis in TNF-α–deficient IL-1Ra$^{-/-}$ mice. Squares, TNF-α$^{+/+}$ IL-1Ra$^{-/-}$ mice (n = 14); triangles, TNF-α$^{+/-}$ IL-1Ra$^{-/-}$ mice (n = 23); circles, TNF-α$^{-/-}$ IL-1Ra$^{-/-}$ mice (n = 23). Statistical significance between genotypes was calculated by repeated-measures ANOVA or two-way ANOVA. *P < 0.01. (**C**) Incidence of arthritis in TNF-α$^{-/-}$ IL-1Ra$^{-/-}$ (Ra$^{-/-}$) or IL-1Ra$^{-/-}$ BM cell–transferred WT mice. Triangles, WT mice transferred with TNF-α$^{-/-}$ IL-1Ra$^{-/-}$ BM cells (T$^{-/-}$Ra$^{-/-}$ → WT); diamonds, WT or heterozygous (IL-1Ra$^{+/-}$) mice transferred with IL-1Ra$^{-/-}$ BM cells (Ra$^{-/-}$ → WT). (**D**) Incidence of arthritis in TNF-α$^{-/-}$ IL-1Ra$^{-/-}$ or IL-1Ra$^{-/-}$ BM cell–transferred IL-1Ra$^{-/-}$ mice. Squares, IL-1Ra$^{-/-}$ mice transferred with TNF-α$^{-/-}$ IL-1Ra$^{-/-}$ BM cells (T$^{-/-}$Ra$^{-/-}$ → Ra$^{-/-}$); circles, TNF-α$^{-/-}$ IL-1Ra$^{-/-}$ mice transferred with IL-1Ra$^{-/-}$ BM cells (Ra$^{-/-}$ → T$^{-/-}$Ra$^{-/-}$).

Identification of cells in the joints and cellular cytokine production. To further analyze the roles of cytokines overexpressed in IL-1Ra$^{-/-}$ T cells, we examined the local subsets of lymphocytes and their cytokine production in the joints. The ankle joints were dissected, and cytokine production in the joint cells was examined by intracellular staining. The total cell number in the ankle joints was increased 2-fold in IL-1Ra$^{-/-}$ mice (7.1×10^6 cells per mouse, n = 10) compared to WT mice (3.7×10^6 cells per mouse, n = 10), suggesting infiltration of inflammatory cells. Thus, although the proportion of T cells was not dramatically increased (Figure 3D), the total T cell numbers in the joints of IL-1Ra$^{-/-}$ mice were greater than in WT mice. In the T lymphocyte subsets, CD4$^+$ cells were detected more frequently than CD8$^+$ cells, consistent with our previous observations (17). We also observed increased infiltration of CD11b$^+$ Gr-1$^+$ cells, most likely activated neutrophils, in the arthritic joints of IL-1Ra$^{-/-}$ mice (Figure 3D).

Cells from the ankle joints were stimulated with PMA and ionomycin to examine the ability to produce cytokines such as TNF-α, IFN-γ, and IL-4. As shown in Figure 3E, most of the IL-1Ra$^{-/-}$ CD11b$^+$ cells produced TNF-α. Some of CD4$^+$ T cells in the joints were also TNF-α–producing cells. Moreover, many more of these cells were found in the IL-1Ra$^{-/-}$ joints, suggesting that the infiltrating CD4$^+$ T cells in arthritic joints may produce more TNF-α and enhance inflammation. Only a small percentage of cells in the joints produced IFN-γ or IL-4 in either WT mice or IL-1Ra$^{-/-}$ mice.

Suppression of arthritis in TNF-α–deficient IL-1Ra$^{-/-}$ mice. We previously reported that high levels of inflammatory cytokines, including TNF-α, were detected in the joints of IL-1Ra$^{-/-}$ mice (9). We also observed TNF-α–producing cells in the ankle joints of these mice (Figure 3E). Furthermore, we detected high levels of TNF-α in the culture of IL-1Ra$^{-/-}$ T cells (Table 2). To elucidate the role of TNF-α in the development of arthritis in IL-1Ra$^{-/-}$ mice, we generated TNF-α and IL-1Ra double-deficient mice by crossing IL-1Ra$^{-/-}$ mice with TNF-α$^{-/-}$ mice.

As shown in Figure 4, A and B, homozygous TNF-α deficiency strongly suppressed development of arthritis in IL-1Ra$^{-/-}$ mice. An intermediate, but significant, suppression was observed in mice heterozygous for the *TNF*-α gene, suggesting a *TNF*-α gene dosage effect on the incidence and severity of arthritis. Histological analyses revealed that TNF-α$^{-/-}$ IL-1Ra$^{-/-}$ mice that appeared normal also showed normal joint histology, but those with swollen joints showed arthritic pathology of inflammation and bone destruction similar to that seen in IL-1Ra$^{-/-}$ mice (data not shown). These results suggest that TNF-α plays critical roles in the development of arthritis in IL-1Ra$^{-/-}$ mice.

However, since the *TNF*-α gene is located in the MHC locus and mice deficient for this gene were produced on the 129 background (H-2^b), TNF-α$^{-/-}$ mice backcrossed to the BALB/c strain (H-2^d) for 8 generations still had the same H-2 locus as the 129 mice. To examine the contribution of the MHC locus in the development of arthritis in IL-1Ra$^{-/-}$ mice, IL-1Ra$^{-/-}$ mice were crossed with the BALB.B congenic for the C57BL/6 H-2 locus (H-2^b) or the B10.D2/n congenic for the BALB/c H-2 locus. The results clearly argued that MHC differences were not responsible for the suppression of arthritis in TNF-α$^{-/-}$ mice (data not shown).

To further analyze the role of TNF-α in the development of arthritis in IL-1Ra$^{-/-}$ mice, we examined the effects of TNF-α deficiency in BM cell transfer experiments. BM cells from TNF-α$^{-/-}$ IL-1Ra$^{-/-}$ mice did not induce arthritis in WT mice up to 30 weeks after transfer, while BM cells from IL-1Ra$^{-/-}$ mice induced arthritis in WT mice starting after 8 to 12 weeks (Figures 2A and 4C). On the other hand, TNF-α$^{-/-}$ IL-1Ra$^{-/-}$ BM cells transferred into IL-1Ra$^{-/-}$ mice induced arthritis, and IL-1Ra$^{-/-}$ BM cells transferred into TNF-α$^{-/-}$ IL-1Ra$^{-/-}$ mice also induced arthritis (Figure 4, C and D). These results suggest that TNF-α produced by both BM-derived cells and non-BM-derived cells plays an important role in the development of arthritis

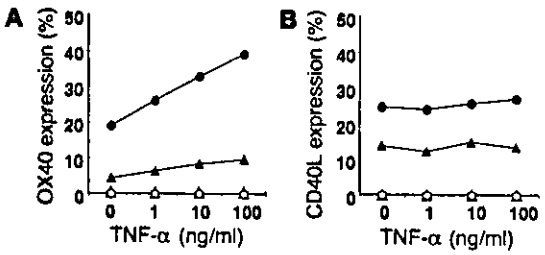

Figure 5

Induction of OX40 expression on T cells by TNF-α. (**A**) OX40 expression (%) on CD4$^+$ T cells stimulated with plate-coated anti-CD3 mAb (0.1 or 0.3 μg/ml) plus TNF-α (0, 1, 10, or 100 ng/ml) for 72 hours. Open symbols: control Ig staining. Filled symbols: anti-OX40 Ab staining for 0.1 μg/ml (triangles) or 0.3 μg/ml (circles) of anti-CD3 mAb stimulation. (**B**) CD40L expression (%) on CD4$^+$ T cells stimulated with plate-coated anti-CD3 mAb (0.1 or 0.3 μg/ml) plus TNF-α (0, 1, 10, or 100 ng/ml) for 24 hours. Open symbols: control Ig staining. Filled symbols: anti-OX40 Ab staining for 0.1 μg/ml (triangles) or 0.3 μg/ml (circles) of anti-CD3 mAb stimulation. Similar results were obtained in 5 independent experiments.

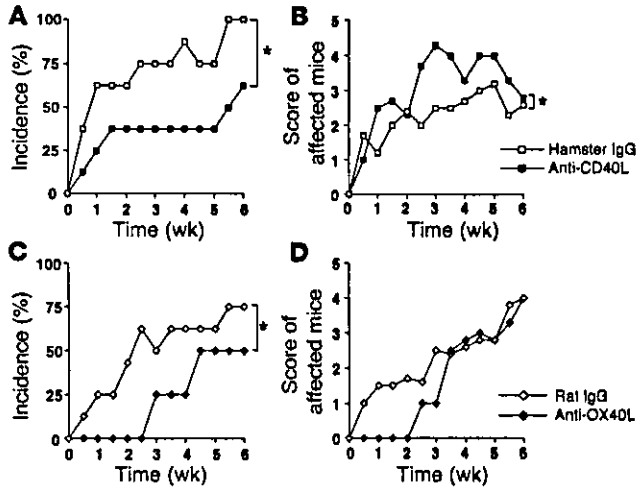

Figure 6
Anti-CD40L or anti-OX40L Ab treatment of IL-1Ra$^{-/-}$ mice. Blocking Abs against either CD40L or OX40L were administrated to IL-1Ra$^{-/-}$ mice before the onset of arthritis. Ab treatment was continued twice a week for 6 weeks, and incidence of arthritis was inspected each time before Ab administration. Incidence and severity score of arthritis in control hamster IgG–treated (open squares, $n = 8$) or anti-CD40L Ab–treated (filled squares, $n = 8$) IL-1Ra$^{-/-}$ mice (**A** and **B**) and those in control rat IgG–treated (open diamonds, $n = 8$) or anti-OX40L Ab–treated (closed diamonds, $n = 8$) IL-1Ra$^{-/-}$ mice (**C** and **D**). *$P < 0.01$ by repeated-measures ANOVA or 2-way ANOVA.

in IL-1Ra$^{-/-}$ mice. Since TNF-α is crucial for the development of arthritis in this model, these results suggest that TNF-α can be produced in the IL-1Ra$^{-/-}$ recipient mice from relatively γ-ray–resistant cells such as macrophages or type A synovial cells.

TNF-α induced expression of OX40, but not CD40L, on T cells. We recently showed that IL-1 produced by APCs induces CD40L and OX40 expression on T cells (15). It has also been reported that ligation between CD40 on APCs and CD40L on T cells leads to TNF-α production from APCs (13). Here we examined the possible involvement of TNF-α in the induction of CD40L and OX40 on T cells. When CD4$^+$ T cells from WT mice were stimulated with varying concentrations of TNF-α (1–100 ng/ml) together with plate-coated anti-CD3 mAb (0–1 μg/ml), the higher concentrations of TNF-α upregulated OX40 expression (Figure 5A), but not CD40L expression, on T cells (Figure 5B). These results suggest that TNF-α may contribute to the development of arthritis in IL-1Ra$^{-/-}$ mice through the induction of OX40 expression on T cells. However, at the highest concentration of anti-CD3 mAb (1 μg/ml), maximal expression of OX40 could occur independent of TNF-α (data not shown).

Involvement of CD40-CD40L and/or OX40-OX40L pathways in the development of arthritis. To explore the contribution of CD40-CD40L and OX40-OX40L pathways to the pathogenesis of arthritis, we injected blocking Abs for these molecules into IL-1Ra$^{-/-}$ mice. Abs for either CD40L or OX40L were injected into IL-1Ra$^{-/-}$ mice for 6 weeks, starting from before onset of the disease, and incidence of arthritis was monitored during the administration period. As shown in Figure 6, Abs for both CD40L and OX40L were able to partially suppress development of arthritis in IL-1Ra$^{-/-}$ mice. The incidence of arthritis was lower in mice treated with anti-CD40L Ab than in those treated with control Ab (hamster IgG) (Figure 6A). The induction of arthritis was delayed in mice treated with anti-OX40L Ab, and the incidence of arthritis after 6 weeks was lower than in mice treated with control Ab (rat IgG) (Figure 6C). However, once arthritis was induced, antibody treatment was ineffective. The severity score of affected mice was similar in anti-OX40L–treated mice and control Ab–treated mice, and severity was actually exacerbated in mice treated with anti-CD40L Ab (Figure 6, B and D). Thus, these results suggest that both the CD40-CD40L and OX40-OX40L pathways are involved in development of arthritis in IL-1Ra$^{-/-}$ mice.

Discussion

In this study, we have shown that the development of arthritis in IL-1Ra$^{-/-}$ mice is completely suppressed in *scid/scid* mice and that IL-1Ra$^{-/-}$ T cell transfers induce arthritis in *nu/nu* mice, suggesting a crucial role of T cells in the pathogenesis of arthritis in this model (Table 1 and Figure 1). T cells from arthritic IL-1Ra$^{-/-}$ mice induced arthritis more efficiently than those from nonarthritic mice, suggesting that arthritogenic-activated and/or memory T cells are generated in IL-1Ra$^{-/-}$ mice and involved in the development of arthritis. However, cells from both arthritic and nonarthritic IL-1Ra$^{-/-}$ mice were able to induce arthritis, supporting a T cell intrinsic defect. Interestingly, donor T cells from IL-1Ra$^{-/-}$ mice are not necessarily primed by autoantigens, because naive T cells from thymus could induce arthritis, although this took longer than with peripheral T cells that may have been preactivated. With regard to this, we have previously shown that IL-1 from APCs can activate T cells through the induction of CD40L and OX40 on T cells (15), and in the absence of IL-1Ra, even physiological levels of IL-1 activate T cells excessively, resulting in the development of autoimmunity (9). Our present data suggest that T cell–derived IL-1Ra also regulates T cell activity in an autocrine manner, although IL-1Ra is known to be produced by many other types of cells, including monocytes and macrophages in the synovial lining layer. In support of this notion, *IL-1Ra* mRNA expression was observed in unstimulated T cells at low levels but stronger expression was induced in activated T cells (Figure 3A). Thus, naive IL-1Ra$^{-/-}$ T cells transferred into *nu/nu* mice may be activated excessively by the endogenous physiological levels of IL-1 which are constitutively expressed in the joints (9), thereby becoming reactive against synovial components.

We showed that transplantation of IL-1Ra$^{-/-}$ BM cells induced arthritis in WT mice, and conversely, introduction of WT BM cells into IL-1Ra$^{-/-}$ mice completely suppressed the disease, indicating that BM cells and their derivatives are abnormal in IL-1Ra$^{-/-}$ mice (Figure 2). Since T cell progenitors are derived from BM cells, these observations are consistent with the notion that T cell dysfunction contributes to the development of autoimmunity. It should be noted, however, that WT mice that received IL-1Ra$^{-/-}$ BM cells took longer to develop arthritis than did nonarthritic IL-1Ra$^{-/-}$ mice that received the same BM cells. Thus, not only the donor BM cells, but also the recipient milieu, seems to be involved in the development of arthritis, suggesting that IL-1Ra from relatively radiation-resistant cells also plays a role. Since the time required for developing arthritis in WT mice that receive IL-1Ra$^{-/-}$ BM cells (3–4 months) is long enough to replace all the BM-derived cells in the recipient mice including the macrophages and type A synovial lining cells in the joint with donor type cells (16), this observation suggests that these late replacing components are involved in the development of arthritis. The observation that it took more than 16 weeks for arthritic IL-1Ra$^{-/-}$ mice that received normal BM cells to recover from the disease also supports this idea.

We have shown that the development of arthritis is completely suppressed in TNF-$\alpha^{-/-}$ mice, indicating a crucial role for TNF-α in the pathogenesis of RA (Figure 4). In this context, a dominant role of TNF-α in the pathogenesis of RA has been demonstrated by recent clinical trials using anti-TNF-α Ab and studies in the mouse using the CIA model (3, 18, 19). It was also reported that transgenic mice carrying the *TNF*-α gene or mice deficient for the TNF-α AU-rich element ($TNF^{\Delta ARE}$), which produce higher amounts of the TNF-α protein, develop arthritis spontaneously (7, 8). However, since $TNF^{\Delta ARE}$ mice develop arthritis even in the absence of mature lymphocytes (8), cells in the innate immune system such as neutrophils, macrophages, and mast cells, rather than the T cell-dependent immune system, have been suggested to be involved in the pathogenesis of this arthritis. Likewise, it has also been reported that inflammatory cytokines such as IL-1 and TNF-α, but not IL-6, play critical roles in the effector phase of the disease in the K/BxN model, in which arthritis can be induced by serum transfer (20). The effect of TNF-α deficiency, however, was not as strong in the CIA and K/BxN models compared to that seen in the IL-$1Ra^{-/-}$ mice. Thus, the IL-$1Ra^{-/-}$ mouse is one of the most sensitive models to the effects of TNF-α.

Cell transfers showed that TNF-$\alpha^{-/-}$ IL-$1Ra^{-/-}$ BM cells could not induce arthritis in WT recipient mice, indicating that BM-derived cells are responsible for the production of TNF-α that is crucial for the development of arthritis. Nonetheless, it is interesting that TNF-$\alpha^{-/-}$ IL-$1Ra^{-/-}$ BM cells could induce arthritis in IL-$1Ra^{-/-}$ recipient mice but not in WT recipient mice. With regard to this, TNF-α expression is augmented in IL-$1Ra^{-/-}$ mouse joints and this TNF-α may compensate for the deficiency in BM-derived cells. It is known that T cells are sensitive to irradiation and synovial lining cells are relatively resistant to irradiation, but some of the synovial lining cells such as the type A cells are of BM origin and are eventually replaced by donor cells after BM cell transplantation. Our results suggest that TNF-α is produced by these synovial lining cells in recipient IL-$1Ra^{-/-}$ mice (Figure 3E). This TNF-α may contribute to the arthritogenic milieu observed in IL-$1Ra^{-/-}$ mice in the IL-$1Ra^{-/-}$ BM cell transfer experiments. Although some $CD4^+$ T cell populations produce TNF-α, it is unlikely that TNF-α produced by these cells is the only source of TNF-α involved in the pathogenesis because, if that were true, TNF-$\alpha^{-/-}$ IL-$1Ra^{-/-}$ BM cells would not have induced arthritis even in IL-$1Ra^{-/-}$ recipient mice. However, since activated IL-$1Ra^{-/-}$ T cells produce high amounts of TNF-α (Table 2 and Figure 3E), it seems likely that T cell–derived TNF-α also contributes to the development of arthritis. Transfer of TNF-$\alpha^{-/-}$ IL-$1Ra^{-/-}$ T cells into *nu/nu* mice will help evaluate this possibility, although we were not able to address this question because of the difference in the MHC locus between the TNF-$\alpha^{-/-}$ and *nu/nu* mice.

We previously showed that IL-1 plays an important role in enhancing T cell–APC interactions by inducing CD40L and OX40 on T cells, and CD40L and OX40 expression were enhanced in T cells stimulated with antigen-bearing IL-$1Ra^{-/-}$ APCs compared to WT APCs (15). It is known that ligation of CD40 on APCs with CD40L induces OX40L expression and TNF-α production by APCs (13, 14). Here, we have shown that TNF-α induces OX40 expression on T cells (Figure 5A). Thus, the mechanism for T cell activation by IL-1 is proposed as follows. Upon interaction with antigens, APCs produce IL-1, and IL-1 activates T cells, resulting in the induction of CD40L. Then, the CD40L-CD40 interaction activates APCs to produce TNF-α. This TNF-α induces OX40 on T cells, leading to enhancement of cytokine production and activation of B cells.

IL-17 plays important roles in inflammatory diseases such as arthritis, contact hypersensitivity, asthma, and delayed-type hypersensitivity (21–23). It was recently reported that a minor subpopulation of activated $CD4^+$ T cells produces both TNF-α and IL-17 (24) and acts in synergy or additively with TNF-α and IL-1 by enhancing their production and action (25). We recently found that IL-17 production from IL-$1Ra^{-/-}$ T cells was induced by OX40 activation, and that IL-17–deficiency completely suppressed development of arthritis in IL-$1Ra^{-/-}$ mice (17). Thus, it is possible that increased OX40 expression on T cells by TNF-α may induce production of IL-17, resulting in exacerbated inflammation.

We show here that blocking CD40-CD40L and OX40-OX40L interactions inhibited the development of arthritis in IL-$1Ra^{-/-}$ mice (Figure 6). These results suggest that blocking molecules downstream of IL-1 and TNF-α in T cell activation may be effective to inhibit development of arthritis in IL-$1Ra^{-/-}$ mice. However, our results showed that once arthritis started, treatment with antibody to CD40L actually exacerbated the progression of the disease (Figure 6B). It was recently reported that activation of CD40-expressing cells has a beneficial effect on the treatment of chronic CIA (26), indicating that not only inhibition of CD40-CD40L interactions, but also CD40 ligation, can be used to reduce the autoimmune inflammatory response. Consistent with this observation, an aggressive form of polyarthritis was described in a patient with a point mutation in the *CD40L* gene (27). Thus, the CD40-CD40L system may play dual functions in the development of arthritis, and blocking the CD40-CD40L interaction by antibody treatment may also prevent beneficial effects of CD40 expression, resulting in exacerbated inflammation in IL-$1Ra^{-/-}$ mice after onset of the disease.

In summary, we have found a novel T cell regulatory mechanism in which IL-1Ra produced by T cells acts on T cells in an autocrine manner. We also showed that IL-1–induced TNF-α is crucial for the development of arthritis in IL-$1Ra^{-/-}$ mice and that this TNF-α induces OX40 on T cells. Furthermore, we showed that inhibition of either TNF-α or OX40 function is effective to suppress the development of arthritis, providing a clue for the development of new therapies for RA.

Methods

Mice. IL-$1Ra^{-/-}$ mice were produced as described (28). TNF-α $^{-/-}$ mice were kindly provided from K. Sekikawa (National Institute of Agrobiological Sciences, Tsukuba, Japan). These mice were backcrossed to the BALB/c strain mice for 8 generations. BALB/c mice, BALB/c-*nu/nu* mice, and BALB/c-*scid/scid* mice were purchased from Clea. B10.D2/n (C57BL/6 congenic) mice were purchased from Japan SLC Inc. BALB.B (BALB/c congenic) mice were provided by T. Shiroishi (National Institute of Genetics, Mishima, Japan). Age- and gender-matched mice were used in each experiment. Mice were kept under specific pathogen-free conditions in an environmentally controlled clean room at the Center for Experimental Medicine, Institute of Medical Science, University of Tokyo, Japan. The animal experiments were approved by the Committee for Animal Experiments of the Institute of Medical Science, University of Tokyo. Gene manipulation experiments were carried out according to the law for such experiments.

Thymocyte, splenocyte, and T cell preparation and transfer. Donor mice for splenocyte or arthritic T cell transfer were between 8 and 12 weeks old, and those for nonarthritic T cell transfer were between 4 and 5 weeks old. Cells were prepared from spleen, thymus, and LNs (axillary, inguinal, branchial,

cervical, and popliteal) as described previously (15). For T cell purification, spleen and LN cells were washed and passed through a nylon wool column, treated with anti-mouse B220 and Mac-1 magnetic beads and passed through a MACS column (Miltenyi Biotec). Purified $CD3^+$ T cells were less than 92% $CD3^+$. Prepared cells were resuspended in 0.2 ml PBS and i.v. transferred into BALB/c-*nu/nu* mice. Numbers of transferred cells per mouse were 10^8 cells for thymocyte transfers, 4×10^7 cells for total splenocyte transfers, and 2×10^7 cells for T cell-depleted splenocyte and T cell transfers.

Incidence of arthritis and the severity score were judged macroscopically and histologically as described previously (9). Briefly, the severity score was judged by eye: grade 0 = normal, grade 1 = light swelling of the joint and/or redness of the footpad, grade 2 = obvious swelling of the joint, and grade 3 = severe swelling and fixation of the joint. The severity score was calculated for all 4 limbs, giving a maximal score of 12 points for one mouse.

BM cell preparation and transfer. Donor mice were between 4 and 8 weeks old. BM cells from femurs, tibiae, and pelves were treated with a hemolysis buffer (17 mM Tris-HCl and 140 mM NH_4Cl, pH7.2) to remove red blood cells. T cells were removed by treating with anti-mouse Thy1.2 magnetic beads and then passed through a MACS column. T cell–depleted and purified BM cells (10^7 cells) in 0.2 ml PBS were i.v. transferred into lethally irradiated (750 rad) recipient mice.

T cell activation, cytokine ELISA, and RT-PCR. $CD4^+$ T cells were purified as described (15). Purified T cells (2×10^5 cells) were plated on a 96-well plate coated with 1 or 10 μg/ml of anti-mouse CD3 mAb (145-2C11; BD Biosciences – Pharmingen) in a final volume of 200 μl RPMI1640 plus 10% FCS and cultured for 48 hours. Culture supernatant was then collected and cell proliferation was measured by incorporation of [^{3}H] thymidine (Amersham Biosciences) (15). IFN-γ, IL-4, and TNF-α levels in culture were measured by ELISA as described previously (22, 29). For the IL-1Ra ELISA, polyclonal goat anti-mouse IL-1Ra (1 μg/ml, R&D Systems Inc.) and polyclonal biotinylated goat anti-mouse IL-1Ra (2 μg/ml, R&D Systems Inc.) Abs were used as capture and detection Abs, respectively. Streptavidin-AP (SouthernBiotech) and substrate (Sigma-Aldrich) were used for detection. Recombinant mouse IL-1Ra (R&D Systems Inc.) was used as a standard. The detection limit was 3.9 pg/ml.

Total RNAs were isolated from BALB/c T cells or T cell–depleted splenocytes using Trizol reagent (Invitrogen Corp.). RNAs were denatured in the presence of oligo (dT)12-18 primer and then reverse transcribed using SuperScript (Invitrogen) at 42°C for 1 hour. PCR was performed for 30 cycles that was within log-phase amplification stages for the PCR products. The primer sequences were as follows: IL-1Ra forward primer, 5′-GACCCTGCAAGATGCAAGCC-3′; IL-1Ra reverse primer, 5′-GAGCGGATGAAGGTAAAGCG-3′; β_2m forward primer, 5′-TGACCGGCTTGTATGCTATC-3′; β_2m reverse primer, 5′-CAGTGTGAGCCAGGATATAG-3′. These IL-1Ra primers detect both secreted and intracellular forms of IL-1Ra.

Intracellular staining of cytokines. For the intracellular staining for IL-1Ra, PECs, or $CD4^+$, T cells were prepared from BALB/c or IL-$1Ra^{-/-}$ mice. PECs were stimulated with LPS (5 μg/ml) for 3 hours, followed by LPS stimulation with 2 μM monensin for 12 hours, then cells were suspended in a staining buffer (PBS containing 2% FCS and 0.01% sodium azide). After blocking with anti-FcγRII/III receptor mAb (BD Biosciences – Pharmingen), cells were treated with FITC-anti-CD11b mAb (BD Biosciences – Pharmingen). Splenocytes were stimulated with soluble anti-CD3 mAb (1 μg/ml), and purified $CD4^+$ T cells were stimulated with plate-coated anti-CD3 mAb (1 μg/ml) for 72 hours, and the GolgiPlug (BD Biosciences – Pharmingen) was added for the final 6 hours of stimulation. Cells were treated with anti-FcγRII/III receptor mAb and stained with cychrome-anti-CD4 mAb (BD Biosciences – Pharmingen). These cells were then fixed with PBS containing 4% paraformaldehyde for 20 minutes. After washing with a permeabilization buffer (PBS containing 10 mM HEPES, 0.1% BSA, and 0.5% Triton X-100), cells were incubated with goat anti-mouse IL-1Ra Ab (R&D Systems Inc.) or isotype-matched control Ab (goat IgG; R&D Systems Inc.) in the permeabilization buffer for 30 minutes at 4°C. Cells were then washed with the permeabilization buffer and stained with Cy5-donkey-anti-goat IgG (Jackson ImmunoResearch Laboratories).

For intracellular cytokine staining for IFN-γ, IL-4, and TNF-α, synovial tissues were dissected from the ankle joints of IL-$1Ra^{-/-}$ mice who had already developed arthritis and normal ankle joints of WT mice. These joints were digested in a cocktail of 2.4 mg/ml hyaluronidase (Sigma-Aldrich), 1 mg/ml collagenase (Wako Pure Chemical Industries) and 100 μg/ml DNase I (Sigma-Aldrich) in RPMI plus 10% FBS for 1.5 hours at 37°C. The cells were filtered through a nylon mesh, washed with RPMI plus 10% FBS, then stimulated with PMA (10 ng/ml) and Ionomycin (400 ng/ml; Sigma-Aldrich) for 6 hours at 37°C with 2 μM monensin. These cells were blocked with anti-FcγRII/III receptor mAb and stained with cell lineage-specific Abs against cell surface molecules, then fixed in 4% paraformaldehyde for 20 minutes, resuspended in the permeabilization buffer, and stained with anti-cytokine Abs for 45 minutes at 4°C. Abs used for the cell lineage-specific staining were as follows: FITC-anti-CD11b, allophycocyanin-anti-TCR-β, CyChrome-anti-CD4, and allophycocyanin-anti-CD8 (BD Biosciences – Pharmingen). Those used for intracellular staining were as follows: PE-anti-IFN-γ, PE-anti-IL-4 (BD Biosciences – Pharmingen), and PE-anti-TNF-α (eBioscience). Cells were washed with the permeabilization buffer and analyzed using FACSCalibur by CellQuest software (BD).

Flow cytometric analysis of costimulatory molecules. CD40L and OX40 expression on $CD4^+$ T cells was analyzed as described previously (15). Briefly, for CD40L expression, purified $CD4^+$ T cells on 12-well plates (1×10^6 cells/well) were stimulated with plate-coated anti-CD3 mAb with or without mouse recombinant TNF-α (Peprotech) in the presence of 1 μg of biotinylated anti-mouse CD40L mAb (MR-1; BD Biosciences – Pharmingen) or biotinylated hamster IgG (eBioscience) as an isotype-matched control Ab for 24 hours. For OX40 expression, $CD4^+$ T cells were stimulated with plate-coated anti-CD3 mAb with or without TNF-α for 72 hours. Cells were stained with allophycocyanin-anti-mouse-CD4 mAb (PharMingen) and either biotinylated anti-mouse OX40 mAb (OX86, eBioscience) or biotinylated rat IgG (eBioscience), followed by staining with PE-streptavidin (BD Biosciences – Pharmingen).

Antibody preparation and treatment. Anti-OX40L Ab and anti-CD40L Ab were produced in hybridoma cell lines, MGP34 and MR-1, respectively. For OX40L Ab preparation, hybridoma cells were allowed to proliferate in ascites of *nu/nu* mice for 7–10 days or cultured in serum-free medium with the iMAb Monoclonal Antibody Production Kit (Diagnostic Chemicals Ltd.) for 4 weeks. Ascites and culture supernatant was collected and Abs were purified using Protein A column (Amersham Biosciences). For CD40L Ab preparation, hybridoma cells were cultured in serum-free medium for 4 weeks. Supernatant was collected and Abs were purified using Protein G column (Amersham Biosciences). Anti-OX40L Ab (500 μg) or anti-CD40L Ab (250 μg) was intraperitoneally injected into nonarthritic IL-$1Ra^{-/-}$ mice twice a week for 6 weeks. Rat IgG or hamster IgG (Cappel, ICN Pharmaceuticals) was injected as the isotype control for anti-OX40L or anti-CD40L Ab, respectively. Mice treated with Abs were between 4 and 6 weeks old. Arthritic score was inspected at the time of Ab injection.

Statistics. The repeated-measures ANOVA-Fisher's protected least significant different test (post hoc test) or the chi-square test for independence was used for statistical evaluation of incidence. The 2-way ANOVA was used for statistical evaluation of the arthritic score. The statistical significance of affected mice scores was calculated from the point at which 2 or more mice of each genotype became arthritic. The Student's *t* test was used for statistical evaluation of the results except for incidence and score.

Acknowledgments

We thank K. Sekikawa for TNF-α$^{-/-}$ mice, T. Shiroishi for BALB.B mice, S. Mori and T. Nakajima (University of Tokyo, Tokyo, Japan) for histological sections, and S.J. Galli (Stanford University School of Medicine, Stanford, California, USA) for support in the experiments. We also thank all the members of the lab for their discussion and help in animal care. This work was supported by grants from the Ministry of Education, Culture, Sport, and Science of Japan; the Ministry of Health and Welfare of Japan; CREST; the Japan Society for the Promotion of Science; and the Japan Rheumatism Foundation.

Received for publication December 5, 2003, and accepted in revised form October 5, 2004.

Address correspondence to: Yoichiro Iwakura, Center for Experimental Medicine, Institute of Medical Science, University of Tokyo, Shirokanedai, Minato-ku, Tokyo 108-8639, Japan. Phone: 81-3-5449-5536, Fax: 81-3-5449-5430; E-mail: iwakura@ims.u-tokyo.ac.jp.

Susumu Nakae's present address is: Department of Pathology, Stanford University School of Medicine, Stanford, California, USA.

Taizo Matsuki's present address is: Japan Science and Technology Agency, Tokyo, Japan.

Katsuko Sudo's present address is: Animal Research Center, Tokyo Medical University, Tokyo, Japan.

1. Feldmann, M., Brennan, F.M., and Maini, R.N. 1996. Role of cytokines in rheumatoid arthritis. *Annu. Rev. Immunol.* **14**:397–440.
2. Firestein, G.S., and Zvaifler, N.J. 1992. Rheumatoid arthritis: a disease of disordered immunity. In *Inflammation: basic principles and clinical correlates*. 2nd edition. J.I. Gallin, I.M. Goldstein, and R. Snyderman, editors. Raven Press, Ltd. New York, New York, USA. 959–975.
3. Feldmann, M., and Maini, R.N. 2001. Anti-TNF-α therapy of rheumatoid arthritis: what have we learned? *Annu. Rev. Immunol.* **19**:163–196.
4. Tocci, M.J., and Schmidt, J.A. 1997. Interleukin-1: Structure and function. In *Cytokines in health and disease*. 2nd edition. D.G. Remick and J.S. Friedland, editors. Marcel Dekker, Inc. New York, New York, USA. 1–27.
5. Iwakura, Y. 2002. Roles of IL-1 in the development of rheumatoid arthritis: consideration from mouse models. *Cytokine Growth Factor Rev.* **13**:341–355.
6. Arend, W.P., Malyak, M., Guthridge, C.J., and Gabay, C. 1998. Interleukin-1 receptor antagonist: role in biology. *Annu. Rev. Immunol.* **16**:27–55.
7. Kollias, G., Douni, E., Kassiotis, G., and Kontoyiannis, D. 1999. On the role of tumor necrosis factor and receptors in models of multiorgan failure, rheumatoid arthritis, multiple sclerosis and inflammatory bowel disease. *Immunol. Rev.* **169**:175–194.
8. Kontoyiannis, D., Pasparakis, M., Pizarro, T.T., Cominelli, F., and Kollias, G. 1999. Impaired on/off regulation of TNF biosynthesis in mice lacking TNF AU-rich elements: implications for joint and gut-associated immunopathologies. *Immunity.* **10**:387–398.
9. Horai, R., et al. 2000. Development of chronic inflammatory arthropathy resembling rheumatoid arthritis in interleukin 1 receptor antagonist-deficient mice. *J. Exp. Med.* **191**:313–320.
10. Niki, Y., et al. 2001. Macrophage- and neutrophil-dominant arthritis in human IL-1α transgenic mice. *J. Clin. Invest.* **107**:1127–1135.
11. Mima, T., et al. 1995. Transfer of rheumatoid arthritis into severe combined immunodeficient mice. The pathogenetic implications of T cell populations oligoclonally expanding in the rheumatoid joints. *J. Clin. Invest.* **96**:1746–1758.
12. Weinberg, A.D. 1998. Antibodies to OX-40 (CD134) can identify and eliminate autoreactive T cells: implications for human autoimmune disease. *Mol. Med. Today.* **4**:76–83.
13. van Kooten, C., and Banchereau, J. 2000. CD40-CD40 ligand. *J. Leukoc. Biol.* **67**:2–17.
14. Weinberg, A.D. 2002. OX40: targeted immunotherapy – implications for tempering autoimmunity and enhancing vaccines. *Trends Immunol.* **23**:102–109.
15. Nakae, S., Asano, M., Horai, R., Sakaguchi, N., and Iwakura, Y. 2001. IL-1 enhances T cell-dependent antibody production through induction of CD40 ligand and OX40 on T cells. *J. Immunol.* **167**:90–97.
16. Kitagawa, H., et al. 1993. Analyses of origin of synovial cells and repairing mechanisms of arthritis by allogeneic bone marrow transplantation. *Immunobiology.* **188**:99–112.
17. Nakae, S., et al. 2003. IL-17 production from activated T cells is required for the spontaneous development of destructive arthritis in mice deficient in IL-1 receptor antagonist. *Proc. Natl. Acad. Sci. U. S. A.* **100**:5986–5990.
18. Thorbecke, G.J., et al. 1992. Involvement of endogenous tumor necrosis factor α and transforming growth factor β during induction of collagen type II arthritis in mice. *Proc. Natl. Acad. Sci. U. S. A.* **89**:7375–7379.
19. Joosten, L.A., et al. 1999. IL-1αβ blockade prevents cartilage and bone destruction in murine type II collagen-induced arthritis, whereas TNF-α blockade only ameliorates joint inflammation. *J. Immunol.* **163**:5049–5055.
20. Ji, H., et al. 2002. Critical roles for interleukin 1 and tumor necrosis factor α in antibody-induced arthritis. *J. Exp. Med.* **196**:77–85.
21. Lubberts, E., et al. 2001. IL-1-independent role of IL-17 in synovial inflammation and joint destruction during collagen-induced arthritis. *J. Immunol.* **167**:1004–1013.
22. Nakae, S., et al. 2002. Antigen-specific T cell sensitization is impaired in IL-17-deficient mice, causing suppression of allergic cellular and humoral responses. *Immunity.* **17**:375–387.
23. Nakae, S., Nambu, A., Sudo, K., and Iwakura, Y. 2003. Suppression of immune induction of collagen-induced arthritis in IL-17-deficient mice. *J. Immunol.* **171**:6173–6177.
24. Infante-Duarte, C., Horton, H.F., Byrne, M.C., and Kamradt, T. 2000. Microbial lipopeptides induce the production of IL-17 in Th cells. *J. Immunol.* **165**:6107–6115.
25. Chabaud, M., and Miossec, P. 2001. The combination of tumor necrosis factor alpha blockade with interleukin-1 and interleukin-17 blockade is more effective for controlling synovial inflammation and bone resorption in an ex vivo model. *Arthritis Rheum.* **44**:1293–1303.
26. Mauri, C., Mars, L.T., and Londei, M. 2000. Therapeutic activity of agonistic monoclonal antibodies against CD40 in a chronic autoimmune inflammatory process. *Nat. Med.* **6**:673–679.
27. Webster, E.A., et al. 1999. An aggressive form of polyarticular arthritis in a man with CD154 mutation (X-linked hyper-IgM syndrome). *Arthritis Rheum.* **42**:1291–1296.
28. Horai, R., et al. 1998. Production of mice deficient in genes for interleukin (IL)-1α, IL-1β, IL-1α/β, and IL-1 receptor antagonist shows that IL-1β is crucial in turpentine-induced fever development and glucocorticoid secretion. *J. Exp. Med.* **187**:1463–1475.
29. Nakae, S., Asano, M., Horai, R., and Iwakura, Y. 2001. Interleukin-1β, but not interleukin-1α, is required for T-cell-dependent antibody production. *Immunology.* **104**:402–409.

Available online at www.sciencedirect.com
SCIENCE DIRECT®
Microbes and Infection 6 (2004) 150–156
Microbes and Infection
www.elsevier.com/locate/micinf

Original article

Regulation of human T-cell leukemia virus type 1 (HTLV-1) budding by ubiquitin ligase Nedd4

Akira Sakurai [a], Jiro Yasuda [a], Hiroko Takano [b], Yuetsu Tanaka [c], Masanori Hatakeyama [d], Hisatoshi Shida [a,*]

[a] Division of Molecular Virology, Institute for Genetic Medicine, Hokkaido University, Kita-15, Nishi-7, Kita-ku, Sapporo 060-0815, Japan
[b] Department of Anatomy, Graduated School of Medicine, Hokkaido University, Kita-ku, Sapporo 060-8638, Japan
[c] Department of Immunology, Graduate School and Faculty of Medicine, University of the Ryukyus, Nishihara, Okinawa 903-0215, Japan
[d] Division of Molecular Oncology, Institute for Genetic Medicine, Hokkaido University, Kita-ku, Sapporo 060-0815, Japan

Received 8 September 2003; accepted 16 October 2003

Abstract

The Gag protein of human T-cell leukemia virus type 1 (HTLV-1) contains the conserved sequences PPxY and PTAP, which are putative viral motifs required for budding (L-domain motifs). We show here that the PPxY motif, but not the PTAP motif, is essential for HTLV-1 virion budding from the plasma membrane. In addition, we show that overexpression of Nedd4 enhances HTLV-1 budding and that Nedd4 interacts with Gag via its WW domain. The HECT domain of Nedd4 is also required for budding. These results indicate that Nedd4 or a Nedd4-related ubiquitin ligase plays a critical role in HTLV-1 budding.

Keywords: HTLV-1; Budding; Nedd4; Ubiquitin

1. Introduction

Retroviral assembly is driven by the Gag precursor proteins. For most of the retroviruses, including human T-cell leukemia virus type 1 (HTLV-1), Gag polyproteins assemble at the plasma membrane, grow a spherical bud form, and are released from the membrane. The HTLV-1 Gag precursor is cleaved by a viral protease into three peptides, termed 19-kDa matrix (MA), 24-kDa capsid (CA) and 15-kDa nucleocapsid (NC). Three functional domains in the Gag protein that are critical for the assembly and budding processes have been identified. The membrane-binding domain (M domain) is required for the myristylation of the Gag N-terminal region and the subsequent targeting of the protein to the plasma membrane. The interaction domain (I domain) appears to be a major region for Gag multimerization. The late assembly domain (L domain) plays a critical role in the pinching off of virus particles from the plasma membrane of infected cells [1–5].

In the Mason–Pfizer monkey virus (M-PMV), Rous sarcoma virus and murine leukemia virus (MuLV), a highly conserved PPxY sequence functions as the core of the L domain [6–8]. In contrast, the human immunodeficiency viruses type 1 (HIV-1) and type 2 (HIV-2) have another crucial motif, PTAP, that acts as the core sequence of the L domain [9,10]. However, the PTAP motif of HIV can be interchanged with other retroviral PPxY motifs without these viruses losing their ability to bud [11,12]. Interestingly, the Ebola virus has overlapping PPxY and PTAP motifs (PTAP-PxY) in the VP40 matrix protein [13], both of which seem to be essential for Ebola viral budding [13,14].

PPxY motifs have been reported to bind to Nedd4-like E3 ligases [7,15,16], suggesting that ubiquitin E3 ligases play an important role in retroviral budding. Supporting this notion is our study showing that expression of a novel Nedd4-like ubiquitin ligase, BUL1, enhances the budding of M-PMV and that when BUL1 is mutated, the ability to bud is lost [17]. The PTAP motif in HIV-1, HIV-2 and the Ebola virus has also been found to interact with a ubiquitin E2 ligase variant (UEV), namely, Tsg101 [4,9,10,18,19]. Recent studies have reported that RNA interference (RNAi) of Tsg101 and the expression of a dominant negative form of Tsg101 block the budding of these viruses [20,21]. Thus, Tsg101 appears to be crucially involved in the budding of some viruses.

* Corresponding author. Tel./fax: +81-11-706-7543.
E-mail address: hshida@imm.hokudai.ac.jp (H. Shida).

doi:10.1016/j.micinf.2003.10.011

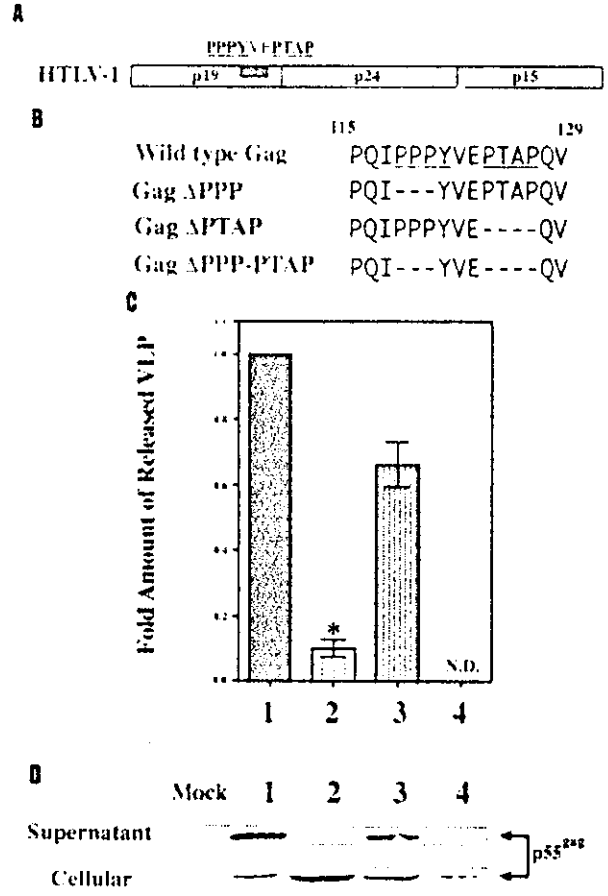

Fig. 1. (A) Location of the PPxY and PT/SAP late domain sequences in HTLV-1. Both the PPxY and PTAP sequences are located in the C-terminal region of the HTLV-1 p19 matrix protein. (B) Schematic representation of the Gag mutants analyzed in this study. (C, D) The PPxY sequence is required for VLP budding. Gag protein in the VLPs and cell lysates was detected by western blotting with the α-p24 antibody (CA). The intensities of the bands for p24 in the VLPs and the cell lysates were quantitated by FLA-3000. The graphical data are presented as the ratio of VLP p24/cellular p24. The extent of VLP budding in wild type was set to 1.0. The data represent averages and S.D. of three independent experiments. Lane 1, wild-type Gag; lane 2, ΔPPPY; lane 3, ΔPTAP; lane 4, ΔPPP–PTAP. The asterisk indicates P value <0.05. N.D., Not detected.

HTLV-1 has both PPxY and PTAP sequences in the MA protein (Fig. 1A), unlike HTLV-2 or the bovine leukemia virus (BLV), which bear only PPxY sequences [22,23]. Therefore, HTLV-1 could bud by using one of three possible mechanisms. First, it could employ the PPxY/E3-mediated pathway like that used by M-PMV. Second, it could bud with the PTAP/UEV-mediated pathway like that in HIV-1. Third, it could use both pathways, as does the Ebola virus. Recently, Le Blanc et al. [26] reported that the PPPY sequence of HTLV-1 was required for the viral budding. However, they did not examine the effect of the PTAP sequence. In this study, we examined which of the HTLV-1 L domain sequences are critical for HTLV-1 budding. We also determined the cellular ligase that is involved in HTLV-1 budding.

2. Materials and methods

2.1. Plasmid

Plasmids that express Nedd4, Nedd4WW, Nedd4C894A, BUL1, KIAA1301, or Tsg101 have been described previously [8,17,24]. To express wild-type and mutant Gag proteins, we used a pJW322 expression vector, which is a pBR322-based plasmid from pJW4303 that includes a CMV promoter. The HTLV-1 *gag* gene was amplified by PCR from HTLV-1 K30, an infectious molecular clone, using a forward primer containing an *Eco*RI site (CGGAATTCCGTCCCTAGGCAATGGGCCAAA) and a reverse primer containing a *Bam*HI site (CGCGGATCCGCGTGTGGGGGGGGAGGTTAAACCT). The amplified product was digested with *Eco*RI and *Bam*HI and cloned into pJW322 to construct the wild-type pGag. Mutated Gag expression vectors were constructed by using QuickChange™ (STRATAGENE) and the wild-type Gag expression vector. The mutated Gag expression vectors, pGag ΔPPP and ΔPTAP, lack the PPP and PTAP sequences of L domain, respectively (Fig. 1B). The pGag ΔPPP–PTAP lacks both the PPP and PTAP sequences (Fig. 1B). The resulting plasmids were verified by sequencing.

2.2. Cell culture and transfection

HeLa cells were cultured in Dulbecco modified Eagle medium, which was supplemented with 10% fetal bovine serum, in a 5% CO_2 atmosphere at 37 °C. Transfection experiments were carried out using LipofectAmine™ 2000 (Invitrogen). The cells were harvested 48 h posttransfection.

2.3. Western blotting

Forty-eight hours after the transfection, the virus-like particles (VLPs) or virions in the culture medium were collected and prepared as previously described [8]. VLPs, virion and cell lysates were resolved by SDS-PAGE, and the proteins were then transferred to nitrocellulose filters. The anti-p24 mouse monoclonal antibody (MAb) NOR-1 [25] or anti-c-myc MAb 9E10 (SIGMA) was used as primary antibody. Horseradish peroxidase- or alkaline phosphatase-conjugated anti-immunoglobulin G (IgG) antibodies (Promega) were used as secondary antibodies. Immunoreactive bands were visualized using ECL+ (Amersham Pharmacia Biotech), followed by the LAS-1000 plus system (Fujifilm) or 5-bromo-4-chloro-3-indolylphosphate-nitroblue tetrazolium solution. For quantitation, the signal intensity on the western blot membrane was evaluated by Image Gauge version 3.4 software (Fuji Film) using the LAS-1000 plus system.

2.4. ELISA

The amount of p19 (MA) in the virion and the cell lysates was quantified using the HTLV-I/II p19Antigen ELISA (ZeptoMetrix).

2.5. Electron microscopy

Transfected 293T cells were fixed with 2% glutaraldehyde in 0.1 M cacodylate buffer for 1 h, postfixed with 1% OsO_4 for 30 min and stained with 1% uranyl acetate for 2 h. After dehydration in a graded series of ethanol (from 80% to 100%), the cells were embedded in Quetol 812. Ultrathin sections (100 nm) were made on MT5000 Ultra-Microtome (Sorvall) and then examined under an H-7100 electron microscope (HITACHI).

2.6. Immunofluorescence microscopy

Transfected 293T cells were fixed with 1% formaldehyde solution, permeabilized with 0.1% NP40, and then stained with the NOR-1 antibody or the α-c-myc polyclonal antibody followed by FITC- or RITC- conjugated secondary antibodies, respectively.

3. Results

3.1. PPxY motif but not PTAP sequence plays an important role in HTLV-1 budding

To determine which motif is critical for HTLV-1 budding, 293T cells were transfected with 0.5 μg of the wild-type or mutated Gag expression vectors, and the VLPs in the culture medium were quantified. To check the expression levels of the Gag protein, we performed western blot analyses, using NOR-1. The VLP release of ΔPPP and ΔPPP–PTAP mutants was severely inhibited, whereas the ΔPTAP mutant showed slight reduction to approximately 65% of the wild type (Fig. 1C). The expression levels of ΔPPP and ΔPTAP Gag proteins were similar to that of wild-type Gag, although ΔPPP–PTAP mutant looked relatively unstable (Fig. 1D). We also constructed the Gag expression vector encoding a mutant form of the PPPY L domain by replacing Pro-118 of pGag wild type with Ala. VLP release of the APPY mutant was reduced similarly to that of ΔPPP mutant (data not shown). In addition, we examined these experiments at different times (24 and 36 h after transfection). Enough the intensity of ELISA signal or western band could not be obtained at 24 h. The experiments at 36 h showed similar results to those of our 48-h experiments (data not shown). Thus, our data suggest that while the PPPY sequence is required for HTLV-1 budding, the PTAP sequence does not play an important role in this process. In addition, we suppose that the reduction in VLP release by the ΔPTAP mutant may be caused by the conformational effect on the PPPY sequence, because only two amino acids exist between the PPPY and PTAP sequences (see Fig. 1A). However, we cannot exclude the possibility that the PTAP sequence has a weak role in HTLV-1 budding. Supporting these observations is the recent report by Le Blanc et al. [26] that the PPPY motif is required for HTLV-1 virion production.

3.2. Morphological examination of ΔPPP and ΔPTAP mutant budding

To further confirm that the PPxY motif but not the PTAP sequence is required for HTLV-1 budding, we examined the budding process of the wild-type and mutated Gag by electron microscopy. Fig. 2A shows the VLPs of wild-type Gag. The VLPs do not have an electron dense core, due to the absence of a viral protease, similar to that of BLV Gag reported previously [23]. In cells transfected with the ΔPPP mutant, no VLPs could be detected in extracellular medium, and the electron-dense thickenings were found on the plasma membrane (Fig. 2C), similar to PPPY point mutants that Le Blanc et al. reported [26]. In cells transfected with the ΔPTAP mutant, VLPs could be detected in extracellular medium, and pinching off formations of Gag were found on the plasma membrane (Fig. 2D,E). These findings indicated that the ΔPTAP mutant of HTLV-1 Gag shows no significant defect in the late assembly step. Thus, these results support the PTAP sequence of HTLV-1 Gag not playing an important role in the HTLV-1 Gag budding process. In contrast, the PPPY motif is suggested to be required for an earlier step of the HTLV-1 budding process than the pinching-off step.

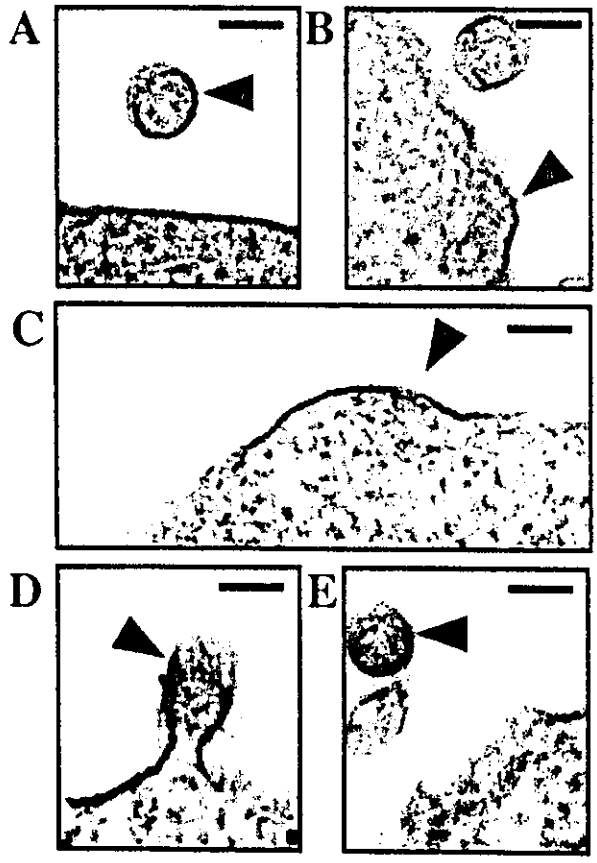

Fig. 2. Electron micrographs of 293T cells transfected with the wild-type or deletion mutant Gag expression vector. (A, B) wild-type Gag. (C) ΔPPP Gag. (D, E) ΔPTAP Gag. Bar: 100 nm.

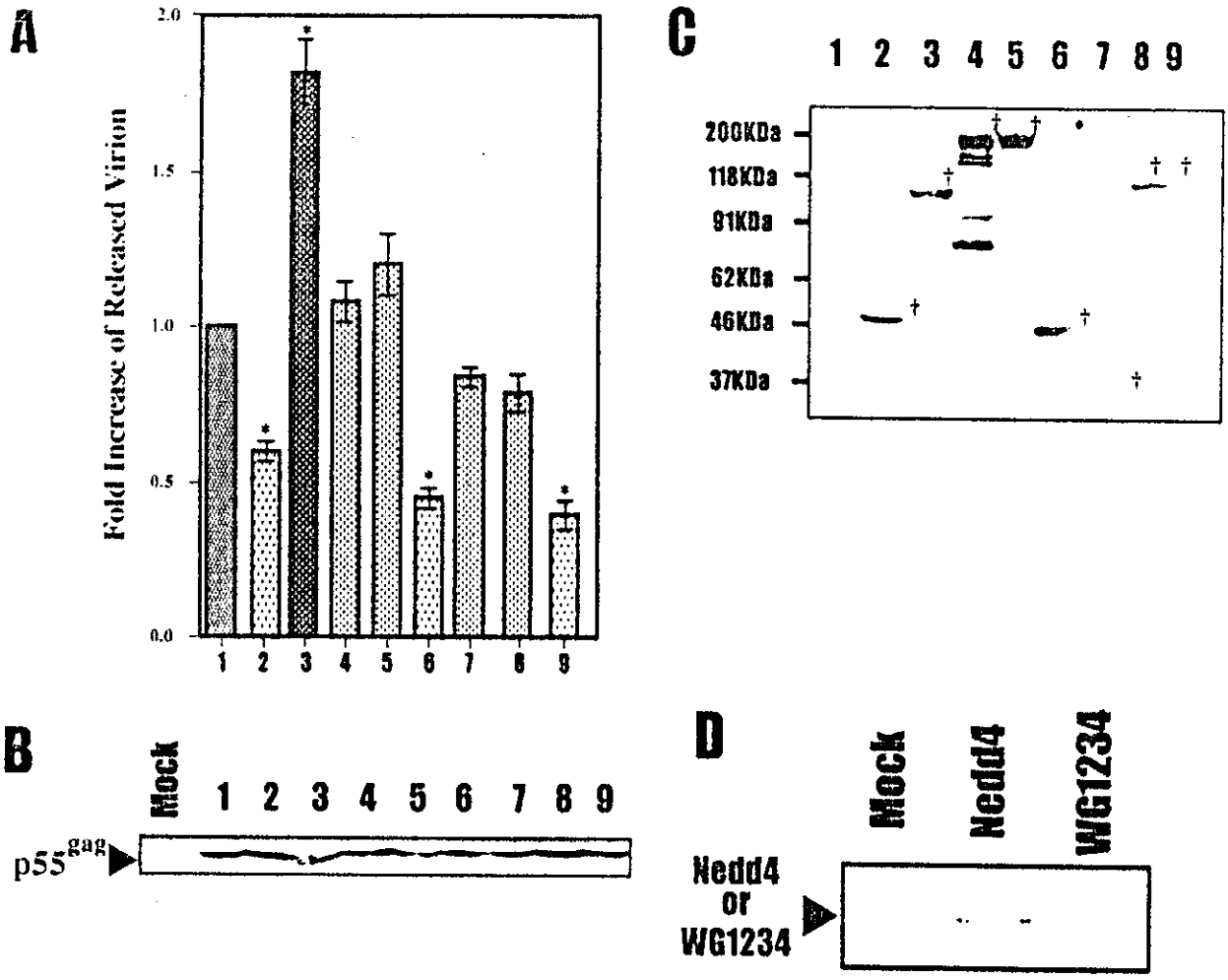

Fig. 3. Effect of overexpressing E3 ligases on HTLV-1 virion release. 293T cells were transfected with pHTLV-1 K30 and the expression vectors of the following molecules: lane 1, control vector; lane 2, Tsg101; lane 3, Nedd4; lane 4, BUL1; lane 5, KIAA1301; lane 6, Nedd4WW; lane 7, BUL1WW; lane 8, Nedd4C894A; lane 9, Nedd4WG1234. (A) The Gag proteins in the virion and cell lysate were quantitated by p19 ELISA. The data are present as the ratio of virion p19/cell p19. The extent of virion budding in wild type was set to 1.0. The data represent averages and S.D. of three independent experiments. The asterisk indicates P value <0.05. The expression levels of Gag protein (B) or E3 ligases (C) in the cell lysates were examined by western blotting with the α-p24 or α-c-myc MAb, respectively. †: the corresponding protein bands. (D) Incorporation of Nedd4 into virions. VLP fractions sedimented by ultracentrifugation were analyzed by western blotting with α-c-myc.

3.3. Overexpression of Nedd4 enhances HTLV-1 budding

The PPxY motif is known to interact with the WW domain [27]. Indeed, we recently reported that the novel ubiquitin ligase BUL1 interacts with the PPPY motif of the M-PMV Gag protein through its WW domain(s) [17]. To examine the involvement of ubiquitin E3 ligase on the egress of the HTLV-1 virus, we overexpressed three kinds of E3 ligases, namely, Nedd4, BUL1 and KIAA1301. Thus, 293T cells were transfected with 0.5 μg of pHTLV-1 K30 and 2.0 μg of each myc-tagged E3 ligase expression vector. Forty-eight hours after transfection, the virions in the culture medium were collected and quantified by ELISA. The p19 levels in the medium were normalized for budding efficiency by the amount of p19 Gag in the cell lysate. Overexpression of Nedd4 enhanced HTLV-1 release, but overexpression of BUL1 and KIAA1301 had little effect on HTLV-1 budding (Fig. 3A). To check the expression levels of the Gag protein and E3 ligases in the transfected cells, we performed western blot analyses with NOR-1 and the anti-c-myc MAb 9E10, respectively. These assays showed that overexpression of the E3 ligases had no pronounced effect on Gag synthesis and stability (Fig. 3B) and that the E3 ligases were efficiently expressed (Fig. 3C). Taken together, these results suggest that Nedd4 or a Nedd4-related E3 ligase plays a critical role in HTLV-1 budding.

3.4. Effect of Nedd4 mutants on HTLV-1 release

To further analyze the regulation of HTLV-1 budding by Nedd4, we constructed several Nedd4 mutants and examined the effect of their overexpression on budding. Nedd4WW expresses only four WW domains composed of the amino acids positioned from 218 to 533. Nedd4WG1234 is a mutant

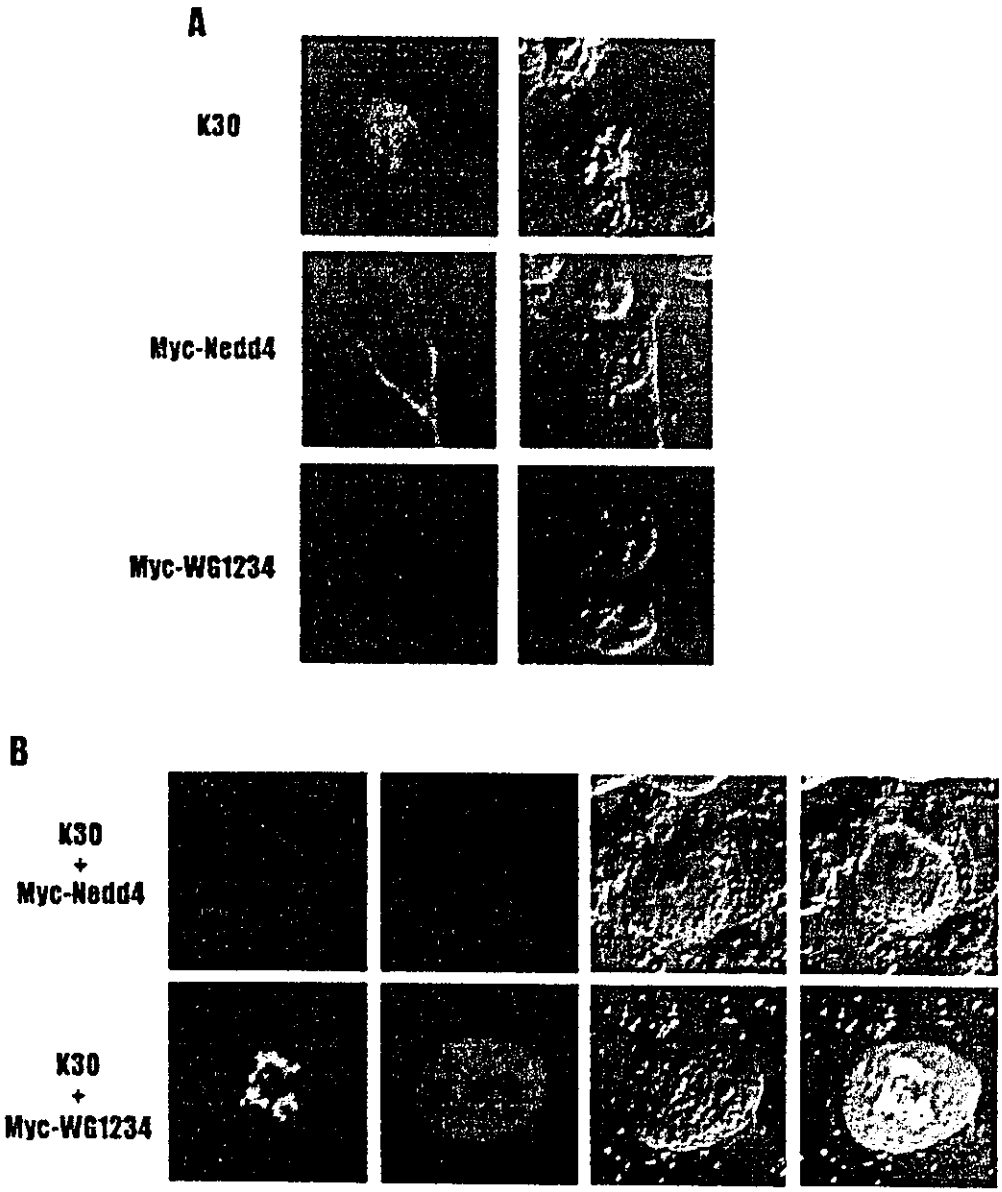

Fig. 4. Localization of HTLV-1 Gag and myc-tagged Nedd4 or Nedd4WG1234. (A) 293T cells were transfected with HTLV-1 K30 (upper) and/or myc-Nedd4 (middle) or myc-Nedd4WG1234 (lower). Gag p24 and the c-myc-tagged protein are stained red and green, respectively. (B) 293T cells were co-transfected with HTLV-1 K30 and the Nedd4 (upper) or the Nedd4WG1234 (lower) expression plasmid.

that has W–G substitutions in all four WW domains. In Nedd4C894A, the critical Cys-894 in the HECT domain has been replaced with Ala [28]. Overexpression of Nedd4WW reduced HTLV-1 release from the cells, while overexpression of BUL1WW, which contains the WW domains of BUL1, had little effect on Gag release (Fig. 3A). Thus, the Nedd4WW domain may interact more strongly with the HTLV-1 PPxY motif than with the BUL1WW domain. Nedd4C894A lost its ability to facilitate virus budding, suggesting that HECT activity is required for the budding function of this protein. Interestingly, Nedd4WG1234 inhibited virion release as much as Nedd4WW. In contrast to Nedd4, overexpression of Tsg101 inhibited the viral budding. To determine whether the release inhibition by overexpression of Tsg101 depends on the PTAP sequence of Gag or not, we transfected 293T cells with 2.0 μg of pBj–Tsg101–myc and 0.5 μg of the wild-type or ΔPTAP Gag expression vectors. Overexpression of Tsg101 reduced the release of VLPs containing ΔPTAP Gag to the same extent as wild-type Gag, (data not shown). Thus, the effect of Tsg101 is independent of interaction between Tsg101 and the PTAP sequence of HTLV-1 Gag.

3.5. Localization of HTLV-1 Gag and Nedd4

Next, to study the effect of overexpressing Nedd4 on Gag localization, we transfected 293T cells with 0.5 μg of pHTLV-1 K30 and 3.0 μg of the Nedd4 or Nedd4WC1234 expression vector and then examined them by immunofluorescence techniques. Nedd4–myc was observed in the cyto-

plasm of the cells when the cells were transfected with the Nedd4 expression plasmid alone (Fig. 4A) [28]. In the cells transfected with pHTLV-1 K30 alone, viral Gag protein was found to localize in both the cytoplasm and the nucleus (Fig. 4A). However, in the cells coexpressing Nedd4 and HTLV-1, the localization of Gag changed to the cytoplasm alone, where it colocalized with Nedd4 (Fig. 4B, upper). Interestingly, Nedd4WG1234 was observed as aggregates in the nuclear or perinuclear region (Fig. 4A) and had no effect on the localization of Gag (Fig. 4B, lower). These results suggest that HTLV-1 Gag specifically binds to the WW domain of Nedd4. This specific interaction between Nedd4 and Gag was also confirmed by the specific incorporation of Nedd4, but not Nedd4WG1234, into virions (Fig. 3D).

We also examined the subcellular localizations of BUL1, KIAA1301 and Nedd4C894A. The two E3s and the Nedd4 mutant were observed in the cytoplasm, and all altered the Gag localization to the cytoplasm to the same extent as wild-type Nedd4 (data not shown).

4. Discussion

Several enveloped viruses, including HTLV-1, MuLV, M-PMV, vesicular stomatitis virus and Ebola virus, bear both a PT/SAP and a PPxY motif in the L domain of the Gag protein [4]. A recent report [26] indicated that the PPPY sequence of HTLV-1 p19 (MA) was required for viral budding. However, they did not examine the effect of the PTAP sequence. In this report, we demonstrated that the PTAP sequence of HTLV-1 p19 was not essential for viral release and that the PPPY motif plays an important role in the budding from membrane. In contrast, the Ebola virus requires both L-domain motifs. Thus, the viruses containing both the PT/SAP motif and the PPxY motif use these L-domain motifs differently in budding. It will be interesting to analyze the functions of the L-domain motifs in the other viruses that have both sequences, as this may help us to better understand the mechanism of virus budding. It may also give clues about the evolution of these viruses.

Overexpression of Nedd4 increased the amounts of HTLV-1 virions, while Nedd4WW inhibited virion release. In addition, other E3 ligases, BUL1 and KIAA1301, had little effect on viral egress. These results suggest that Nedd4 or a Nedd4-related E3 ligase plays a critical role in HTLV-1 budding. Previously, we showed that BUL1, but not Nedd4, enhances the PPxY-mediated budding of M-PMV [17]. Thus, viruses containing a PPxY motif in the L domain seem to utilize different E3 ligases in the viral budding step.

Interestingly, Nedd4WG1234 also inhibits HTLV-1 budding, although it does not compete with endogenous Nedd4 for binding to Gag. Since the mutant was observed to aggregate in the cytoplasm, it is conceivable that Nedd4WG1234 may alter the subcellular localization of other critical cellular factors such as E2 ubiquitin ligase, which results in the inhibition of virus budding.

In the cells coexpressing Nedd4 and HTLV-1, Gag was localized to the cytoplasm only, and colocalized with Nedd4. On the other hand, overexpression of Nedd4WG1234 had no effect on Gag localization. These results indicate that Nedd4 interacts with HTLV-1 Gag via its WW domain(s). Overexpression of BUL1, KIAA1301 and Nedd4C894A also altered the Gag localization, although these E3s do not affect HTLV-1 budding. These results indicate that the interaction of an E3 ligase with the PPxY motif of Gag via the WW domains is necessary but not enough for virus budding. Thus, a region(s) other than the WW domains, such as the HECT domain, may be required to facilitate the budding function of Nedd4. Particularly, C894A mutation in Nedd4 abolished the function of this ligase in HTLV-1 viral budding, which suggests that the enzymatic activity of Nedd4 as a ubiquitin ligase may be essential for viral budding.

Overexpression of Tsg101 had an inhibitory effect on HTLV-1 budding irrespective of the presence of the PTAP motif in the Gag. Recently, Goila-Gaur et al. [29] reported that overexpression of Tsg101 inhibits HIV-1 release in a manner independent of the interaction between HIV-1 Gag and Tsg101. Taken together, overexpression of Tsg101 may inhibit HTLV-1 budding by disturbing the multivesicular body (MVB) sorting pathway. Moreover, Garrus et al. [21] consistently reported that a dominant negative mutant of VPS4, which plays an important role in the MVB sorting pathway, inhibited the budding not only of HIV-1 but also of MuLV. MuLV bears the PPxY motif as its L domain, whereas HIV-1 uses PTAP [9,10]. Thus, the MVB sorting pathway may be required for the budding of both PPxY- and PT/SAP-bearing viruses. We propose that the PPxY-dependent budding of various viruses may utilize a specific E3 ligase(s) during the first steps, after which budding is continued using a process such as the MVB sorting pathway, which is also employed by PT/SAP-bearing viruses.

Acknowledgements

We thank Kantou Nakajima, Tsubasa Ohta and Junko Hioki for their excellent technical assistance. This work was supported by grants from the Ministry of Education, Sports, Science and Technology (MEXT) of Japan, the Japan Society for the Promotion of Science (JSPS), the Japan Health Science Foundation (JHSF), and the Ministry of Health, Labour and Welfare of Japan. The infectious molecular HTLV-1 clone K30 was obtained through the AIDS Research and Reference Reagent program.

References

[1] M.A. Accola, B. Strack, H.G. Gottlinger, Efficient particle production by minimal Gag constructs which retain the carboxy-terminal domain of human immunodeficiency virus type 1 capsid-p2 and a late assembly domain, J. Virol. 74 (2000) 5395–5402.

[2] E.O. Freed, Viral late domains, J. Virol. 76 (2002) 4679–4687.